Novel Acridine–Triazenes as Prototype Combilexins: Synthesis, DNA Binding, and Biological Activity

Adrian W. McConnaughie† and Terence C. Jenkins*

Cancer Research Campaign Biomolecular Structure Unit, The Institute of Cancer Research, Sutton, Surrey SM2 5NG, U.K.

Received October 18, 1994®

A series of bifunctional ligands has been developed as prototype DNA-binding combilexins using a DNA template-directed approach. These novel agents contain a 1,3-diaryltriazene linker moiety, present in the established DNA minor groove-binder berenil [1,3-bis(4′-amidinophenyl)-triazene], which is attached to an intercalating acridine chromophore by a functionalized thiazole residue. This 9-arylacridine is predicted to confer rotational freedom to the hybrid molecule and thus facilitate bifunctional interaction with double-stranded DNA through a combination of 'classical' intercalation and minor groove-binding processes. The noncovalent DNA-binding properties of these acridine–triazene combilexins, together with the component molecular fragments, have been examined by fluorescence quenching and thermal denaturation studies with calf thymus DNA and two oligonucleotides, $[poly(dA\text{-}dT)]_2$ and $[poly(dG\text{-}dC)]_2$. In addition, the binding behaviors of these acridine compounds are compared to those of proflavine (3,6-diaminoacridine) and its 9-phenyl derivative. The results indicate that the hybrid agents (i) are more DNA-affinic than either molecular component, (ii) retain the AT-preferential binding properties of the parent *di*functionalized 1,3-diaryltriazene residues, despite *weak* GC-preferential behavior associated with the acridine chromophore, and (iii) have a reduced binding affinity at pH 7 that reflects the protonation status of the acridine. In contrast, the more basic proflavines show much greater binding affinity and a marked preference for GC-rich DNA sequences. *In vitro* cytotoxicity data with L1210 mouse leukemia and A2780 human colon cancer cell lines show that the conjugate molecules are ~10–40-fold more potent than the acridine or triazene subunits and have activities that compare favorably with those of other reported synthetic combilexins. Intercalative binding modes with a model d(GATACGATAC)·d(GTATCGTATC) target duplex have been investigated using molecular modeling techniques. These studies provide a rational basis for the binding properties and suggest that the prototype combilexins can bind in a bimodal manner that induces little distortion of the host DNA duplex. Energy-minimized models for the possible dual interactions are discussed.

Introduction

The search for more effective anticancer agents has focused to a large extent on the design of molecules capable of recognizing and binding to target DNA base sequences.[1] Such ligands offer a potential means of controlling gene, and especially oncogene, expression by inhibiting or competing with the sequence-specific binding of regulatory proteins to genomic DNA and/or interfering with transcription processes.[2] As a consequence, several design approaches have been exploited in the quest for novel and effective recognition agents.[1b]

Selective control of gene function is currently being assessed using synthetic oligonucleotides targeted toward either mRNA (antisense approach) or duplex DNA (antigene strategy).[3] Nevertheless, low molecular weight molecules that bind to double-stranded DNA in a nonintercalative, sequence-directed manner continue to be an alternative focus of attention.[4] However, high-resolution NMR, X-ray crystallography, molecular modeling, and DNA footprinting studies have shown that most neutral or cationic agents of this class, particularly noncovalent ligands, bind preferentially to AT-rich sequences in the minor groove of B-DNA (see, for example, refs 5–10).

Recent approaches to the design of DNA-binding compounds capable of recognizing heterogeneous DNA sequences have included bifunctional molecules (combilexins) containing linked intercalative and minor groove-binding moieties.[11] In this strategy, the coupling of a groove binder with a DNA-affinic intercalating chromophore provides a basis for modulating the sequence-selective binding behavior and/or tailoring the hybrid ligands for mixed-sequence recognition. Ideally, this latter feature would require the intercalant to exhibit a measure of GC site specificity rather than sequence-neutral binding. Natural molecules that bind to DNA in a reversible, bifunctional manner include the antitumor agents actinomycin D, echinomycin, and the anthracyclines.

Synthetic combilexins based upon a phenoxazone intercalant and two minor groove-binding ligands, netropsin and distamycin, have been reported.[12] Further examples have been developed, including (i) a simple acridine linked to netropsin and distamycin analogues,[13] (ii) a series of agents with 9-anilinoacridine linked to lexitropsin (e.g., NetGA) or SPKK oligopeptide units,[14] (iii) an ellipticine–distamycin derivative,[15] and (iv) an oxazolopyridocarbazole–netropsin derivative (Net–OPC).[16]

In this article we report the design and synthesis of a series of hybrid acridine combilexins, where the

* Address correspondence to this author at CRC Biomolecular Structure Unit, The Institute of Cancer Research, Cotswold Rd., Sutton, Surrey SM2 5NG, U.K. Telephone: (44)-181-643-8901, ext 4255. Fax: (44)-181-770-7893. e-mail: t.jenkins@icr.ac.uk.

† Present address: Laboratory of Molecular Biology, Hills Rd., Cambridge CB2 2QH, U.K.

® Abstract published in *Advance ACS Abstracts*, August 1, 1995.

0022-2623/95/1838-3488$09.00/0

intercalative chromophore is combined with a distal, functionalized 1,3-diaryltriazene moiety to provide secondary interaction with the DNA minor groove. Berenil [1,3-bis(4'-amidinophenyl)triazene, 'diminazene'] is an archetypal DNA-binding agent with antiprotozoal and antiviral properties.[4,17] Extensive biophysical studies have shown that this crescent-shaped molecule binds preferentially to AT-rich tracts in the minor groove of duplex DNA with favored binding sites consisting of three to four consecutive A·T base pairs (bp),[7,8,10] although a recent NMR study has shown that a spanned G·C pair can be tolerated.[10c] Removal of one or more amidine group in berenil, or replacement with a carbonyl residue, results in diminished binding affinity and attenuation of the AT-selective behavior,[10] while the introduction of cationic functions leads to a restoration of binding activity (T. C. Jenkins, unpublished results).

The prototype combilexins described (**16**–**23** in Scheme 2) retain the linear 1,3-diaryltriazene linkage present in berenil, necessary for a isohelical fit within the DNA minor groove[18] and to provide favorable hydrophobic interaction with the groove walls.[7,8] In contrast to berenil, however, the hybrid molecules are essentially monofunctionalized with regard to the remote protonatable residue, with the 'berenil analogue' **18** bearing a single amidine group. Thus, the acridine component in the hybrid agent can be regarded as a formal replacement for one of the amidine residues in the parent berenil molecule. Replacement functional groups for the terminal amidine residue have also been examined, including neutral ketone and amide functions (**16** and **17**), together with basic ω-aminoalkyl benzoate esters (i.e., **19**–**23**). This is the first report of synthetic combilexins that do not contain a lexitropsin or oligopeptide as the minor groove-binding component.

The diaryltriazene moiety is attached to the planar acridine chromophore through a functionalized thiazoleethanol group. This linkage was selected following molecular modeling and quantum mechanical studies, as the 5-membered ring permits facile rotation about the (acridine)C9–aryl bond, without steric hindrance due to atomic clash of *o*-H atoms with the acridine H-1/8 protons. Thus, interplane torsion angles of ~20–30° can be achieved due to a low energy barrier, in contrast to six-membered aromatic systems (e.g., 9-phenyl) where the orthogonal arrangement is favored. Flexibility at this junction is essential for delivery of substituents intended to interact with the groove, as the groove walls are effectively oriented at ~40° relative to the mean intercalation plane in B-DNA. The thiazole-$(CH_2)_2O$- linker was judged to be optimal for attachment of a 1,3-diaryltriazene through a 4-carboxylate ester, allowing the substituents to protrude into either groove of the DNA duplex template upon intercalation of the acridine. This molecular skeleton represents a rational alternative framework for connection to replace the ubiquitous 9-amino- or 9-anilinoacridine linkage developed from the antileukemic agent *m*-AMSA. Details of the drug design and energy calculations will be described elsewhere.

DNA-binding results are presented for the combilexins and the separate component molecules with calf thymus DNA and two polyoligonucleotide duplexes. *In vitro* cytotoxicity data against two cell lines are described. The prototype combilexins are compared to proflavine (3,6-diaminoacridine) and its 9-phenyl derivative **28** to examine the effects of ring substituents upon DNA-binding affinity, groove delivery of the aryl group, and possible site-selective intercalation. The increased basicity of proflavine would be predicted to enhance binding as effective intercalation is likely to require *N*-protonation of the aromatic chromophore. Results from a molecular modeling study with a defined DNA sequence are described, illustrating a possible interaction mode with double-stranded DNA and providing a qualitative basis for bifunctional binding by these novel composite agents.

Chemistry

Commercially available thiazole **1** was selected as a starting point for the synthesis, with the ethanol moiety acting as a two-carbon linker between the 9-arylacridine chromophore and the pendant minor groove-binding function. The adopted strategy involves the 4-aminobenzoate ester **6** as a synthon for the target 1,3-diaryltriazenes. Our initial synthetic approach to **6**, via the corresponding nitro ester **5**, is shown in Scheme 1.

Catalyzed protection of **1** with 3,4-dihydro-2*H*-pyran (DHP) gave the *O*-tetrahydropyranyl derivative **2** in essentially quantitative yield. Thiazole **2** was subsequently deprotonated using 1-butyllithium and treated with 10-alkylacridinone **3**;[19] acidic workup of the addition product furnished 9-(2-thiazolyl)acridine **4** in good yield, and subsequent acylation gave the nitrobenzoate **5**. However, catalytic hydrogenation of **5** led to simultaneous reduction of the nitro group and the acridine ring system. ^{1}H-NMR analysis revealed formation of aminoacridan **7** due to the appearance of two singlets at 5.71 and 6.26 ppm, corresponding to the H-9 and H-10 acridan ring protons, respectively. TLC examination indicated similar rates of reduction for the competing reduction steps, preventing isolation of the target amino ester **6**. Equivalent facile hydrogenation of the acridine ring was observed for **4** and 9-phenylacridine.

The alternative strategy used for the amino ester **6** and the triazene combilexins is shown in Scheme 2. Treatment of **8** with mesitylenesulfonyl chloride (MtsCl) in refluxing acetone gave sulfonamide **9** in good yield. Base-catalyzed coupling of **9** with alcohol **4** using 1,3-dicyclohexylcarbodiimide (DCC) gave the protected ester **10** in good yield. Subsequent deprotection by treatment with methanesulfonic acid at room temperature gave amine **6** in essentially quantitative yield, without cleavage of the ester function. Diazotization of **6** and coupling with the appropriate substituted aniline gave the target triazenes **16**–**23** in moderate yield. Anilines **11**–**15**, used in the preparation of triazenes **19**–**23**, were synthesized (Table 1) by esterification of the appropriate aminobenzoic acid as shown in Scheme 2.

9-Phenylproflavine (**28**) was synthesized via the fully protected acridinone **26** (Scheme 3). Thus, treatment of 3,6-diaminoacridinone **24**[20] with ethyl chloroformate gave bis(carbamate) **25** in good yield, and subsequent trisalkylation with NaH/MEM chloride provided acridinone **26**. Grignard addition of PhMgCl to **26**, followed by mild acidic workup, gave the 9-phenyl bis(carbamate) **27**; cleavage with aqueous HBr afforded proflavine **28** in good yield. Bis(sulfonamide)-protected acridinone **26** represents a novel and useful synthon for the hitherto

Scheme 1[a]

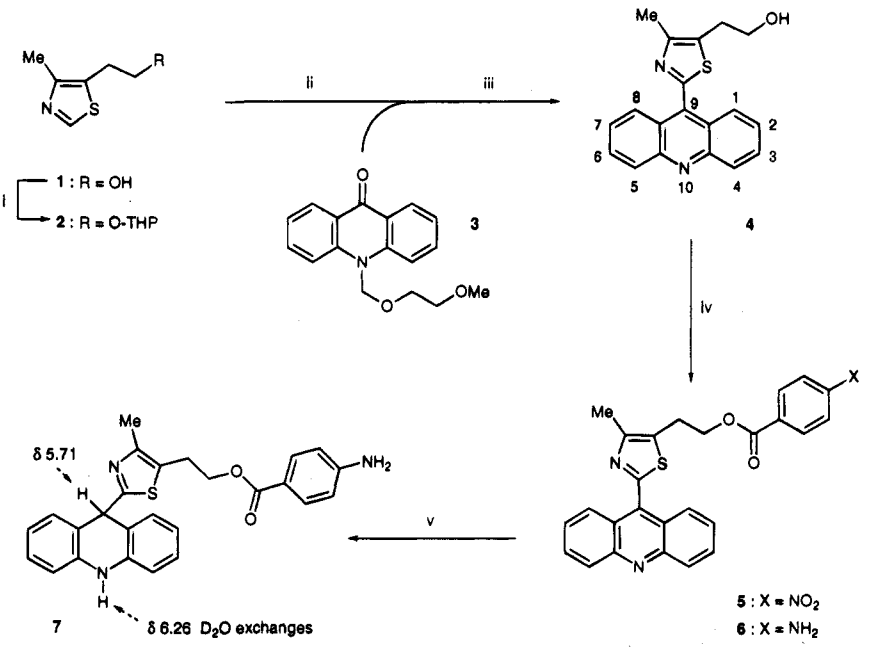

[a] Reagents: (i) DHP/4-TsOH/Δ; (ii) *n*-BuLi/THF/−78 °C, then acridinone **3**;[19] (iii) HCl/EtOH/Δ; (iv) 4-nitrobenzoyl chloride/CH_2Cl_2/pyridine/Δ; (v) H_2/Pd−C/THF/rt.

inaccessible 9-substituted proflavines. Selected properties for the combilexins are collected in Table 1.

Results and Discussion

DNA-Binding Properties. Thermal denaturation data for interaction of the hybrid acridine−triazenes **18**−**23**, acridine derivatives, and parent berenil analogues with calf thymus DNA (CT-DNA) and the oligomers [poly(dA−dT)]$_2$ and [poly(dG−dC)]$_2$ are shown in Table 2. The results show that these agents stabilize the thermal helix → coil transition (T_m) for the CT-DNA duplex at pH 6.0, albeit to only a small extent. Correspondingly smaller positive ΔT_m values were determined for CT-DNA at pH 7.0, indicating that *N*-protonation of the acridine chromophore to the acridinium species (cf. pK_a for acridine = 5.6) leads to more effective binding. By comparison, proflavine and **28** stabilize CT-DNA to a much greater extent at both pH values, reflecting the increased basicity of the 2,6-disubstituted chromophore (cf. pK_a for proflavine = 9.7) and hence greater affinity for the polyanionic DNA duplex. The phenyl substituent in **28** weakens binding to CT-DNA by 30−40% relative to proflavine. A similar effect is evident for acridine and 9-phenylacridine (Table 2), suggesting that the introduction of an aryl group leads to general destabilization of a DNA−acridine or DNA−acridinium complex but does not prevent intercalation. Equivalent effects are observed for binding to [poly(dA−dT)]$_2$ and [poly(dG−dC)]$_2$.

The ΔT_m values determined for the simple 9-arylacridines resemble that of acridine itself. However, comparison of ΔT_m data for **4** and **6** with values for combilexins **18**−**23** shows that elaboration of the acridine side chain leads to a progressive increase in the strength of binding, with the hybrid molecules providing the greatest differential stabilization. Biphasic rather than monophasic DNA melting behavior was seen with several compounds (Table 2), suggesting possible secondary modes of interaction for these ligands. Reliable T_m values could not be determined for **16**−**18** due to thermal instability, particularly at low pH or with the high-melting GC-containing nucleic acids, as observed for other functionalized diaryltriazenes including **32** and **33** (unpublished results). Precipitation and/or ligand-induced aggregation similarly prevented determination of T_m values for **6** and **19** with [poly(dG−dC)]$_2$ at the concentrations used in this assay.

Generally small ΔT_m shifts were obtained for the GC-containing synthetic polynucleotide with all compounds, suggesting that the stabilization of thermal denaturation is reduced at high temperatures. However, possible preferential binding for combilexins **19**−**23** is indicated from the markedly different drug-induced effects upon the low- and high-temperature portions (AT and GC segments, respectively) of the melting curves with the 'pseudorandom' CT-DNA native sequence (not shown). While not conclusive, this behavior suggests that AT-containing sequences are likely to be favored for binding.

The positive ΔT_m shifts for hybrid monofunctionalized ligands **19**−**23** are intermediate between the values determined for acridine and the doubly functionalized 1,3-diaryltriazenes, although the values are small compared to those reported for other synthetic combilexins, including a netropsin−acridine derivative (NetGA in Table 2),[14a] Net−OPC,[16] and anilinoacridine−SPKK compounds.[14c] The superior stabilizing effects of the parent berenil and **30** molecules when compared to **29** is in part due to poor basicity associated with the morpholine function, as **29** will be only ~10% protonated at pH 7 whereas both berenil and **30** are fully diprotonated at physiological pH. The DNA-binding affinities of diaryltriazenes have been shown to be strongly pH-dependent, particularly where protonatable amine or amidine functions are present (unpublished results).

Fluorescence quenching assays employing bound ethidium and an excess of [poly(dA−dT)]$_2$ can be used to distinguish intercalating agents from nonintercalative ligands, as the latter exert a greater effect due to their inherently larger DNA-binding site sizes.[21] Competitive

Scheme 2[a]

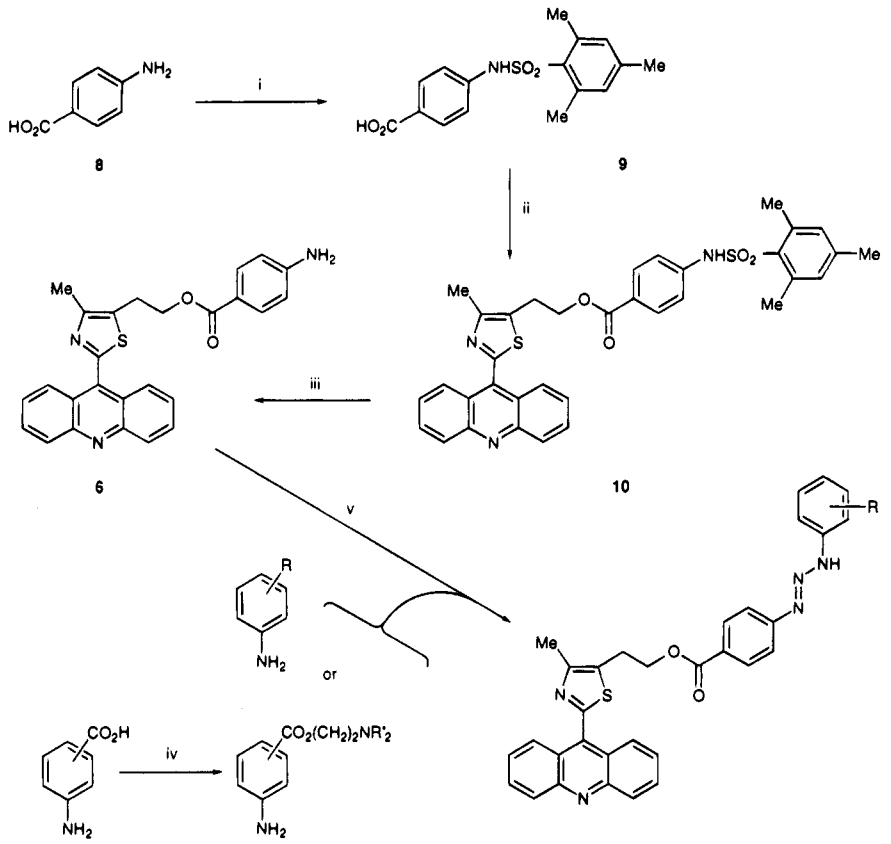

[a] Reagents: (i) MtsCl/CH_2Cl_2/pyridine/Δ; (ii) alcohol **4**/DCC/THF/Δ; (iii) CH_3SO_3H/rt; (iv) $ClCH_2CH_2NR_2$/acetone/K_2CO_3/Δ; (v) $NaNO_2$/HCl (aq), 0–5 °C, then 3- or 4-aniline, pH 7.

Scheme 3[a]

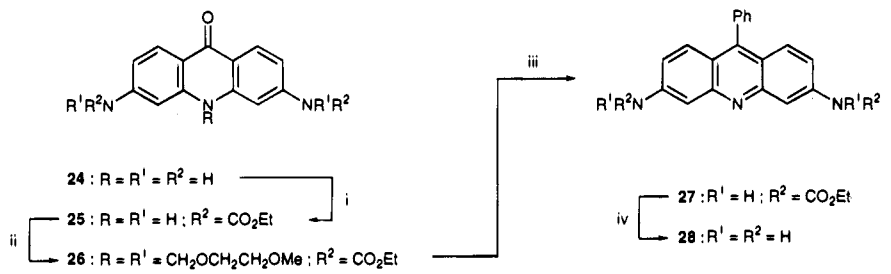

[a] Reagents: (i) EtOCOCl/Δ, then HCl (aq)/MeOH/Δ; (ii) NaH/DMF, then MEM chloride; (iii) PhMgCl, then HCl (aq)/EtOH/Δ; (iv) HBr (aq)/Δ.

(CC_{50}) assays involving displacement of DNA-bound fluorochrome ethidium at a considerably higher [ethidium]:[DNA] ratio facilitate the determination of 'apparent' equilibrium constants (K_{app}) for drug binding, as the CC_{50} value is approximately inversely proportional to the binding constant.[22] Such K_{app} values have been shown to correlate with computed interaction enthalpy for a wide spectrum of minor groove-binding ligands, particularly where the host DNA duplex contains an AT tract of suitable length to accommodate the molecule.[23]

In the present study, fluorescence quenching and displacement assays were performed at pH 5 to ensure that the added drugs were present predominantly as the cationic species, as in previous acridine studies.[14a,22b] The CC_{50} values (Table 2) determined for ethidium displacement from CT-DNA by combilexins **16–23** indicate that the hybrid molecules, particularly base-functionalized agents **18–23**, are strong DNA-binding ligands with affinities similar to that of berenil but 23–120-fold greater than that of acridine. Thus, K_{app} values of (2.1–10.5) × 10^6 M^{-1} for **18–23** compare with 8.9 × 10^4 M^{-1} for acridine and (1.9–2.9) × 10^6 M^{-1} for the parent berenil analogues. In contrast, the neutral ketone and amide combilexins **16** and **17** are markedly less affinic with activities that approach those of the simple parent acridines, in agreement with the dimin-

Table 1. Properties of the Aniline Esters 11–15 and Triazene Combilexins 16–23

compd	mp (°C)	yield[a] (%)	formula	anal.[b]
11	119.5–120.5	62	$C_{13}H_{18}N_2O_3$	C, H, N
12	94–95	72	$C_{14}H_{20}N_2O_2$	C, H, N
13	97–98	48	$C_{13}H_{16}N_2O_2$	C, H, N
14	120–121	75	$C_{11}H_{16}N_2O_2$	C, H, N
15	84.5–85.5	60	$C_{11}H_{16}N_2O_2$	C, H, N
16	227–228.5 dec	26	$C_{34}H_{27}N_5O_3S$	C, H, N, S
17	230–232 dec	46	$C_{33}H_{26}N_6O_3S \cdot 1.5H_2O$	C, H, N, S
18	192–194 dec	54	c	c
19	195–197 dec	38	$C_{39}H_{36}N_6O_5S \cdot 0.5H_2O$	C, H, N, S
20	163–165 dec	34	$C_{40}H_{38}N_6O_4S$	C, H, N, S
21	94–96 dec	35	$C_{39}H_{36}N_6O_4S \cdot 0.5H_2O$	C, H, N, S
22	153–155 dec	62	$C_{37}H_{34}N_6O_4S \cdot H_2O$	C, H, N, S
23	115–118 dec	32	$C_{37}H_{34}N_6O_4S \cdot 1.2H_2O$	C, H, N, S

[a] Yields are unoptimized. [b] Indicated elemental analyses are within ±0.4% of the theoretical values. [c] Characterized by NMR and HRMS.

ished binding predicted for unprotonated carbonyl-functionalized derivatives.[10] Similarly, CC_{50} values of ≥150 μM were determined for **31** and the monofunctionalized triazenes **32** and **33**, indicating reduced binding affinity. On this basis, we infer that the 9-thiazolylacridine residue in the hybrid ligands (e.g., **18**) behaves as an effective replacement function for *one* of the amidine residues of berenil and must contribute to the overall binding process.

The quenching (Q) values for combilexins **16–23** with [poly(dA–dT)]$_2$ are intermediate between those for acridine/proflavine and the berenil analogues (Table 2), with the behaviors of **19** and **20** resembling those of the difunctionalized counterparts **29** and **30**, respectively. Thus, the Q value for **18** is ~2-fold higher than for the bis(amidine) berenil but indicates that it is considerably more effective than acridine itself. As noted from the displacement assays, the quenching activities of the neutral ketone and amide **16** and **17** more closely resemble that of the acridine component. The intercalator compounds, including acridine derivatives **4** and **6** and *m*-AMSA,[14a] are clearly less effective than either the hybrid composite molecules or the simple diphenyltriazenes. These results indicate that a minor groove-binding mode, rather than a strict intercalative process, is implicated for the hybrid ligands. Thus, we conclude from the T_m and ethidium displacement data that *both* modes of interaction must be involved in the overall binding by these ligands.

The Q values determined using native or synthetic DNAs of different base composition can give information relating to their base- or sequence-preferential binding.[14a] Table 2 reveals that the conjugate ligands **16–23** show enhanced affinity for the poly(dA–dT) duplex with some ~3-fold AT specificity, as observed for berenil and the difunctionalized analogues. In contrast, the simple acridines show favored binding to [poly(dG–dC)]$_2$, with a weak GC specificity that increases to ~2-fold in the case of proflavine. The binding behavior seen for the acridine chromophores is less marked than for *m*-AMSA[14a] but is in accord with a reported weak preference of proflavine for GC-rich DNA sequences.[24] These results indicate that the triazene structure fragment of the hybrid molecules exerts a dominating role in the binding process, leading to overall AT specificity. This finding is in agreement with recent competition studies and results for other synthetic combilexins, where the intercalating acridine or ellipticine chromophores have little influence upon the overall sequence recognition properties.[11,14a,25]

Footprinting experiments with a *tyrT* duplex DNA fragment were not conclusive as to base sequence preference since the hybrid ligands **16–23** do not give a distinct footprint and inhibit cleavage by DNase I, even at low concentration (K. R. Fox, unpublished results). In certain cases, drug-induced precipitation of the DNA fragment provided further experimental difficulty. The failure to give a distinct pattern of cleavage may result from fast dissociation of the ligand from the DNA–drug complex, as has been suggested for *m*-AMSA.[26] Attempted viscometric studies to determine DNA helical lengthening induced by the acridine residue were similarly thwarted due to problems associated with aggregation or precipitation (W. D. Wilson, personal communication). The intercalative component of binding for the composite molecules is hence assumed from the behavior established for the parent acridine chromophores.

Cytotoxic Activity. *In vitro* cytotoxic activity was determined for the acridines and combilexins using the human A2780 colon cancer cell line (Table 2). Cytotoxic potency was also evaluated using L1210 leukemia cells for the hybrid compounds, and the component acridine and symmetric diaryltriazene molecules (i.e., berenil, **29**, and **30**), to enable comparison with other reported combilexins. Similarly, both **24** and **28** were examined and compared to the parent proflavine.

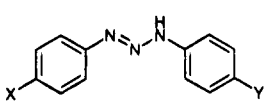

berenil : X = Y = $C(NH)NH_2$
29 : X = Y = $CO_2(CH_2)_2N$(4-morpholine)
30 : X = Y = $CO_2(CH_2)_2N$(1-piperidine)
31 : X = Y = H
32 : X = H ; Y = $C(NH)NH_2$
33 : X = H ; Y = $CO_2(CH_2)_2N$(1-piperidine)

Table 2 shows that acridine and the simple 9-arylacridines, including **4**, **6**, and acridinone **24**, are essentially inactive toward both cell lines. Similarly, neither berenil nor the functionalized diaryltriazenes **29** and **30** show significant cytostatic potency. Weak cytotoxic activity is general for both symmetric and unsymmetric 1,3-diphenyltriazenes, particularly for monofunctionalized derivatives (e.g., IC_{50} values of >150 μM for **31–33** and 44 μM for the symmetric triazene equivalent of **22** in L1210 cells). In marked contrast, the acridine–triazene combilexins **17–23** show good cytotoxic potency in both cell lines, such that the hybrid agents are ~10–40-fold more toxic than either of the component molecular fragments. Only the hybrid acetophenone **16** shows poor activity (see below).

Compounds **17–23** represent the most potent hybrid agents from this series, with cytotoxic activities that compare favorably with behavior reported for other combilexins with L1210 cells, including netropsin–anilinoacridine agents (ID_{50} = 0.5–8 μM; e.g., NetGA),[14a] netropsin–OPC derivatives (CC_{50} = 3–37 μM),[27] and hybrid SPKK compounds (IC_{50} = 2–5 μM).[14c] However, such hybrid ligands remain much less cytotoxic than established DNA intercalants, including *m*-AMSA and adriamycin.[14]

In qualitative agreement with DNA-binding data, the hybrid combilexins with protonatable basic side chains generally confer greater cytotoxic activity, particularly

Table 2. DNA-Binding[a] and *in Vitro* Cytotoxicity Data for the Acridines, Triazenes, and Hybrid Combilexins **16–23**

	Q (μM)[b]				induced ΔT_m shift (°C) at pH 6.0[d]				inhibitory IC_{50} concn (μM)[e]	
compd	AT	CT-DNA	GC	CC_{50}[c] (μM)	AT	CT-DNA	CT-$DNA_{pH\ 7.0}$	GC	L1210	A2780
acridine	26	24	22	142	0.7	1.7	0.7	0.8	45	>100
9-phenylacridine	23	22	18	175	0.6	1.3[f]	0.4	0.4	80	>100
4	22	21	19	190	0.7	1.0	<0.2	<0.2		>100
6	24	20	17	230	0.8	1.1[f]	0.4[f]	*g*		>100
16	19	25[h]	33[h]	123		*g*			100	>100
17	21	26[h]	36[h]	96		*g*			28	5.3
18	12	18	31	2.9	2.4	*g*	*g*	*g*	66	16
19	17	28	39	6.1	0.9	2.4[f]		*f*	32	2.6
20	14	27	52	3.2	1.9	2.4	1.5	0.2	6.2	3.9
21	15	26	45	2.8	1.5	2.9	1.4	0.3	3.4	3.5
22	16	35	66	3.6	1.7	3.0[f]	1.8[f]	<0.2	3.2	3.1
23	14	17	34	1.2	1.6	2.1[f]		<0.2	3.0	3.8
proflavine	24	20	14		24.4	16.4	11.5	7.0	2.7	0.47
24									67	>100
28	22	19	16		20.3	11.7	6.9	3.3	2.0	1.2
berenil	5	9	19	4.4[i]		9.3[j]	7.9[j]		32	
29	14	15	17	6.8		3.6	1.4		>100	
30	11	13	14	5.7		14.5	7.7		>100	
NetGA[k]	5.5	7	12		5		3		8[l]	
m-AMSA[k]	25	3.8	4.5	8.9[m]	4		1		0.05[l]	0.1

[a] AT, CT-DNA, and GC refer to [poly(dA-dT)]$_2$, calf thymus DNA, and [poly(dG–dC)]$_2$, respectively. [b] Drug concentration to give 50% quenching of fluorescence of bound ethidium at an added [ethidium]:[DNA] molar ratio of 0.1:1 (see text); mean value (±1 μM) from three determinations. [c] Drug concentration to give 50% drop in fluorescence of bound ethidium at an added [ethidium]:[CT-DNA] molar ratio of 1.26:1 (see text); mean value (±5%) from three determinations. [d] Mean value (±0.1–0.2 °C) from three determinations for a [drug]:[DNAp] ratio of 1:5. [e] Drug concentration required to inhibit cell growth by 50% after 48 h (L1210) or 96 h (A2780). [f] Biphasic melting. [g] Measurement prevented by aggregation or thermal decomposition effects. [h] Extrapolated value due to precipitation at high ligand concentrations. [i] CC_{50} = 1.4 μM at pH 7.4 in Tris buffer, from ref 23. [j] Values determined for a [drug]:[DNAp] ratio of 1:20. [k] ΔT_m values measured at pH 7.0 with a [drug]:[DNAp] ratio of 1:10 (from ref 14a). [l] Following drug exposure for 24 h (from ref 14a). [m] Data from ref 22b.

in the L1210 cell line. Thus, the reduced relative activities of **16**, **17**, and **19** (Table 2) are suggested to reflect the neutral ketone or amide pendant groups and the weak basicity of the morpholine residue, respectively. The uniformly poor biological activity of 'berenil' combilexin **18** is attributed to problems due to aggregation in aqueous media; experimental difficulties with the neutral ketone **16** similarly contributed to a reduced activity. No compound from this study had a significant influence upon the relative resistance of a derived cisplatin-resistant A2780 cell line.

The 9-aryl derivative **28** shows good toxicity with both cell lines, comparable to proflavine itself, but ≥40-fold higher activity compared to 9-phenylacridine. Thus, the introduction of this substituent in **28** does not seriously diminish the activity of proflavine (Table 2), suggesting that proflavine analogues of these combilexins may offer superior biological potency.

Molecular Modeling. In view of the favored GC binding of the parent acridines and AT-preferential binding of the conjugate molecules indicated from our fluorescence studies, we have examined the interactions of these ligands with DNA using a model d(GATACGATAC)·d(GTATCGTATC) duplex (Figure 1). This core sequence, with an embedded 5′-CpG intercalation site flanked on each side by a 3-bp A/T base stretch, has been used in molecular modeling studies to examine the conformation and dynamics of DNA–proflavine intercalation.[28] Further, this asymmetric sequence, derived from an earlier crystallographic study, provided a source of high-quality atomic coordinates suitable for an extended DNA complex. This 10-mer duplex was selected for modeling purposes solely on the basis of the binding behaviors of the ligands, reflecting the availability of sites suitable for dual CpG intercalation and AT-specific groove binding. However, it should be noted

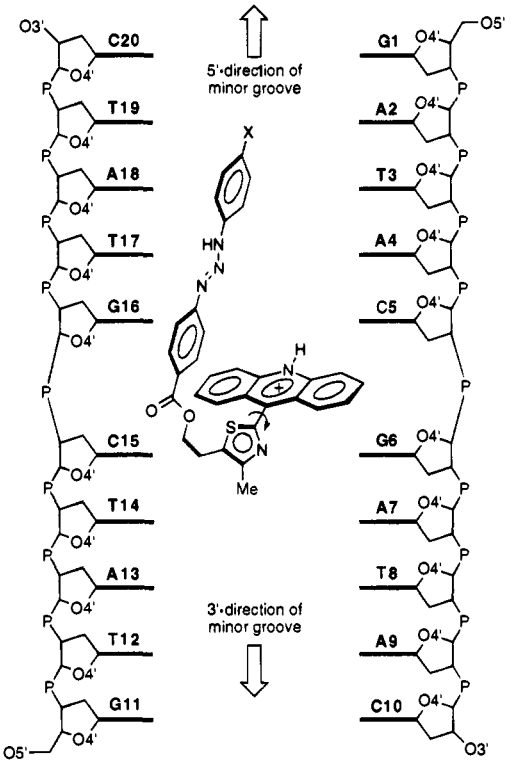

Figure 1. Schematic representation of bifunctional complex formation with the combilexins, viewed looking into the minor groove and showing the numbering system used for the DNA.

that this particular sequence may not represent the optimal sequence for binding with the composite ligands.

Replacement of the ligand molecule in the reported low-energy DNA–proflavine complex[28] with the candidate acridine, using a molecular overlay procedure, facilitated construction of model complexes for energy minimization and subsequent comparison. Where fea-

Table 3. Binding Energies (kcal/mol) for Intercalation of the N10-Protonated Acridinium Salts with d(GATAC·GATAC)·d(GTATC·GTATC)[a]

	E_{bind} for possible drug alignments[c]			
compd[b]	5′-minor	3′-minor	5′-major	3′-major
acridine	−31.4 (−16.4)		−27.5 (−14.9)	
9-phenyl-acridine	−40.2 (−16.2)		−26.9 (−14.4)	
4	−54.1 (−38.7)	−51.3 (−32.3)	−34.2 (−19.3)	−36.5 (−16.8)
6	−50.9	−43.6	−35.1	−35.2
16	−57.7	−56.5	−32.3	−34.9
17	−59.8	−58.5	−33.4	−35.6
18	−74.4	−73.4	−42.2	−47.6
19	−66.8	−65.3	−46.0	−48.1
20	−71.6	−70.8	−46.7	−48.4
21	−70.3	−68.5	−48.4	−50.6
22	−69.1	−68.6	−46.2	−49.3
23	−67.9	−67.0	−47.8	−50.5
proflavine	−53.1 (−39.8)		−34.8 (−27.1)	
28	−46.7 (−39.3)		−32.5 (−31.3)	

[a] C·G denotes an embedded 5′-CpG intercalation site (see text). [b] Values in parentheses refer to N10-unprotonated acridine ligands. [c] Alignment of the acridine 9-substitutent relative to the 5′-GATAC·GATAC strand.

sible, alternative ligand alignments with respect to the DNA host were examined, with (i) the acridine N10 ring atom directed toward either the minor or major groove and (ii) the attached C9 substituents directed toward either the 5′- or 3′-end of the DNA in the corresponding major or minor groove. Thus, two distinct DNA–ligand complexes were evaluated in the case of the symmetric acridine compounds, whereas four complexes, differing solely in groove location for the 9-substituent, were examined for asymmetric ligands **4**, **6**, and **16**–**23**. The effects of protonation at the N10 acridine ring position and, where possible, in the basic side chains were also examined for selected molecules.

Table 3 indicates that all the ligands can form stable, low-energy complexes by intercalation with a model DNA duplex. More stable complexes are formed with an N10-protonated acridinium species than the free base acridines, with a 7–24 kcal/mol increase in binding energy for the most energetically favored complexes. This result is consistent with the pH-dependent binding behavior (Table 2) and confirms that unprotonated acridines are poor DNA intercalants.

The effect of ligand orientation is only weak for unsubstituted acridine free base, with an enthalpy difference of <2 kcal/mol in favor of an intercalated complex where the N10 heteroatom is directed toward the major rather than minor groove. This energy difference increases to ~4 kcal/mol upon N10 protonation, although the favored orientation remains unaltered. Interestingly, proflavine is computed to bind to this DNA with the exocyclic amino groups positioned in the major groove, for both neutral and N10-protonated species, in agreement with crystallographic studies.[28,29] Proflavine is predicted to bind more strongly than simple acridine by ~22 kcal/mol for both the free base and the favored acridinium species, in accord with our T_m results.

For all 9-arylacridines examined (Table 3), the most energetically favorable complexes are formed with the attached aromatic moiety positioned within the minor rather than major groove and with the N10 atom of the intercalated chromophore directed toward the major groove. Analysis of the energy components (not shown) indicates that this results from (i) generally superior nonbonded contacts with the floor and walls of the minor groove and (ii) reduced perturbation of the DNA base pairing in the vicinity of the intercalation site. Thus, the 9-phenyl group attached to acridine effects ~9 kcal/mol further stabilization in the most favored complex, although the equivalent proflavine → **28** mutation is destabilizing by ~6 kcal/mol due to partial disruption of the favorable major groove wall contacts for the DNA–proflavine complex. Interactions between the arene substituents and the DNA bases are mostly weak, although the flexible ethanol group in **4** provides ~3 kcal/mol further stabilization due to H-bonded contact with sugar O4′ acceptor atoms in the minor groove.

Superior binding enthalpies are computed for the hybrid combilexins **16**–**23** (Table 3), where the most favored interactions appear for ligands with protonatable amine or amidine functions in the distal side chain. Thus, the rank order **18** > **20**–**23** > **19** broadly reflects the basicity of the basic residues, whereas the lower E_{bind} values for **16** and **17**, bearing neutral substituents, resemble the energies computed for the less elaborate acridines, including **6**. These conclusions are in qualitative agreement with the binding behavior and biological potency determined for the agents (Table 2). Protonation of the side chain amine groups in combilexins **19**–**23** was shown to improve the enthalpy of interaction by 14–19 kcal/mol.

The 9-aryl substituents are accommodated within the DNA minor groove in an isohelical fashion and induce little distortion of the helix other than a slight widening of the minor groove due to 'clamping' of the ligand. Thus, the berenil analogue **18** spans a 4-bp tract adjacent to the intercalation site, whereas the more extended ligands **19**–**23** effectively span a 5-bp base sequence. In the latter cases, close (ligand)N-H···DNA contacts are formed involving H-bond acceptor nucleotides. Minor groove orientation of the distal substituents appears to have little influence for this DNA duplex (Table 3), with binding thus predicted to favor 5′-GATACpG (≡5′-CpGTATC) rather than 5′-CpGATAC (≡5′-GTATCpG) by only ~2 kcal/mol.

The lowest-energy DNA–ligand complexes achieved for **18** and **22** are shown in Figures 2 and 3, respectively. In each case, the planar acridine chromophores are well stacked within the CpG intercalation site and the thiazole rings are rotated by ~25° from coplanarity. Interestingly, the alkyl substituents on the thiazole ring are directed along the path of the minor groove but do not make contact with the groove walls. The thiazole-CH_2CH_2OCO linker appears to be almost optimal for delivery of a 1,3-diphenyltriazene, such that low-energy near-type-I complexes[10a] are formed, with the central nitrogen atom of the triazene effectively positioned in the plane of a base pair. The two phenyl rings are oriented toward the floor of the minor groove in a parallel alignment with the groove walls and with the inner-facing atoms making close hydrophobic contact with the A3–C5·G16–T18 segment. Snug isohelical fit is achieved by concerted right-handed torsional rotation of the phenyl rings, such that twist angles are ≤12°. In the case of **18** (Figure 2), good H-bonded contacts are achieved with T3(O2) and T3(O4′) acceptor atoms, at (amidinium)N-H···O separations of 1.89 and 1.95 Å, and subtended angles of 143° and 151°, respectively. In contrast, **22** (Figure 3) makes a single contact with A2-

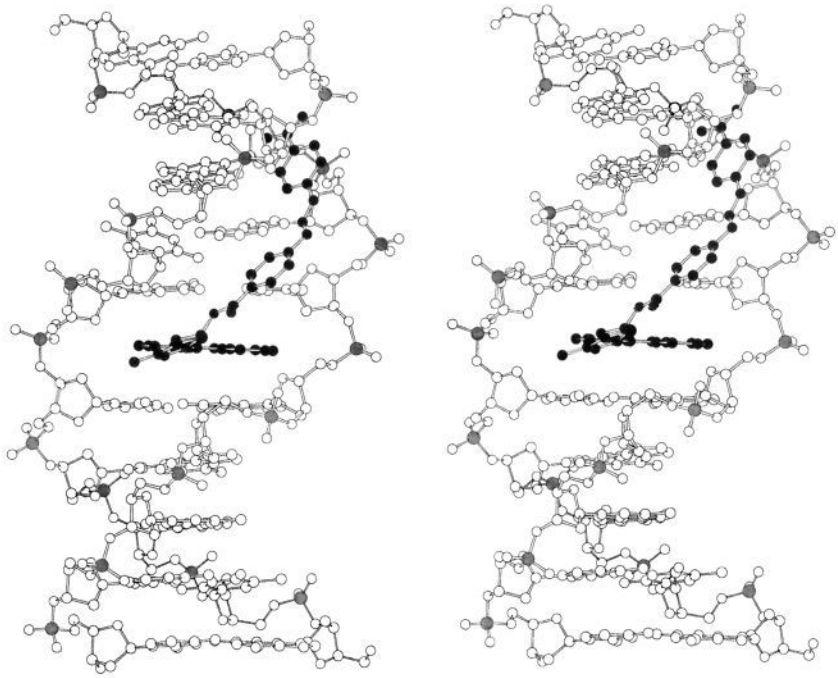

Figure 2. Stereoview of the lowest-energy DNA–**18** complex looking into the DNA minor groove and showing the alignments of the thiazole and 1,3-diaryltriazene residues. All H atoms have been removed for clarity. The combilexin molecule is highlighted, and the DNA backbone phosphorus atoms are shown stippled.

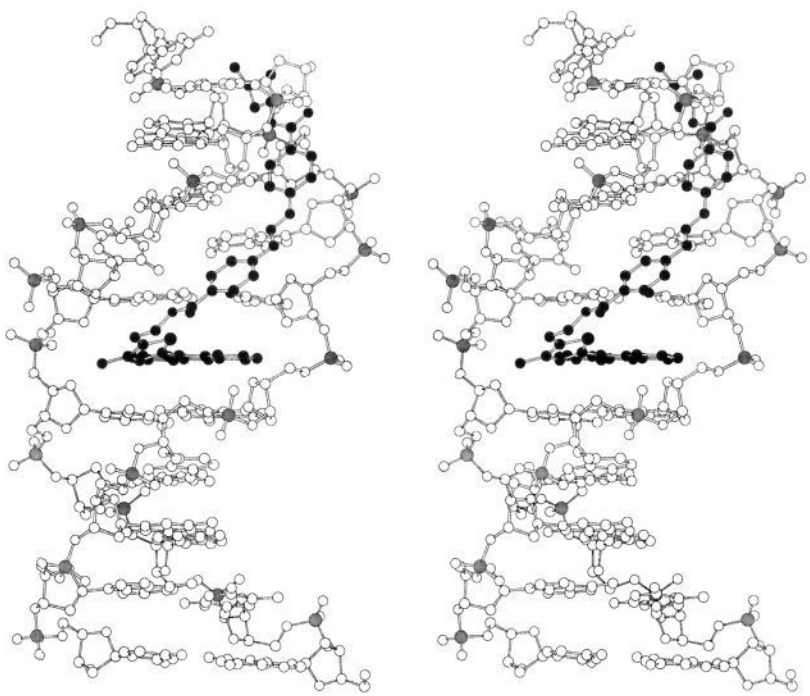

Figure 3. Stereoview of the energy-minimized DNA–**22** complex looking into the DNA minor groove. All H atoms have been removed for clarity. The hybrid ligand molecule is highlighted, and the DNA backbone phosphorus atoms are shown stippled.

(O4′), with an excellent H-bonded geometry, such that the (amine)N–H···O separation is 1.92 Å and the subtended angle is 171°. Neither molecule induces significant perturbation of the host DNA duplex, although the extended **22** ligand causes a partial 5′-end fraying that would be ameliorated by using a longer model sequence. Further, **22** induces an increased propeller twist for the A4·T17 base pair, caused by localized ligand-induced helical compression, but this effect is not propagated.

Previous modeling studies of DNA complexes with a netropsin–acridine hybrid (NetGA)[11] and a distamycin–ellipticine conjugate ('Distel')[15] indicate that bifunctional binding can be achieved with snug accommodation of the lexitropsin functions within the minor groove. However, bimodal binding with either ligand induces pronounced helical bending toward the minor groove in the vicinity of the intercalation site, leading to localized deformation (for a review, see ref 11). In marked contrast, the acridine–triazene combilexins are pre-

dicted to induce negligible base pair disruption or conformational perturbation of the DNA, suggesting that the linker function used is here sufficiently flexible to prevent distortion effects and possible mutual interference between the two binding components.[25b]

Conclusions

This study has shown that a DNA template-directed strategy can be used to develop novel hybrid molecules designed to interact with the DNA duplex through a bimodal association process: (i) intercalation of an acridine chromophore and (ii) simultaneous minor groove binding of an attached monofunctionalized diaryltriazene moiety related to berenil. Fluorescence-based studies confirm that these combilexins have a strong binding affinity for DNA, with K_{app} values of (2.1−10.5) × 10^6 M^{-1} for binding of **18**−**23** to CT-DNA. However, this behavior is sensitive to the protonation status of the acridine intercalant as stronger binding is seen at lower pH values; both proflavine and **28** bind avidly to DNA at pH 7 due to effective N10 protonation of the more basic chromophore.

The binding data clearly demonstrate that the composite agents are more DNA-affinic than either of the separate monofunctionalized molecular component fragments, with activities that resemble or exceed those of their difunctional berenil analogues. Significantly, this result indicates that a suitably substituted acridine can compensate for removal of one cationic function from the parent 1,3-diaryltriazene derivative (e.g., berenil → **18** or **30** → **20**), where such groups largely dictate their behavior as minor groove-binding ligands. Tethering to an intercalant in this way could be expected to assist with anchorage, particularly if the conjugated entities exert negligible mutual effect on the binding processes and do not induce conformational changes that may impede binding by either component.[11,25]

One goal of this study was to examine the sequence-selective binding of the hybrid molecules and to establish whether the intercalant residue has a modulating influence on the AT-preferential minor groove binder. The spectroscopic studies reveal that the combilexins show a preference for AT base tracts rather than GC-rich sequences, with a selectivity that is dominated by the 'berenil-like' component despite a *weak* GC specificity associated with the acridine. Similar retention of AT specificity is also reported for lexitropsin-based combilexins, where the intercalant moieties have no marked effect upon the sequence-selective binding of the linked groove-sensing component.[11]

Preliminary molecular modeling studies with a model DNA sequence confirm that a bimodal interaction is energetically feasible. Energy-minimized complexes of the combilexins indicate a snug isohelical fit of the distal triazene function within the minor groove, good base stacking with the intercalated acridine, and, importantly, no gross helical distortion. Further, the computed binding energies show that superior binding is realized for an N10-protonated chromophore and, preferably, also with a cationic distal side chain function. This model provides a good qualitative structural basis for the solution-binding properties. Binding to AT tracts will be preferred due to energetically favorable H-bonded and nonbonded intermolecular contacts, whereas GC binding will be strongly disfavored by steric clashes with the exocyclic guanosine 2-NH_2 groups.[7,8,10] However, as our DNA footprinting experiments were unsuccessful, further discussion of base sequence selectivity and the molecular interactions involved must await NMR or crystallographic structural studies with oligonucleotide duplexes of defined sequence.

In vitro evaluation of the acridine−triazenes reveals good cytotoxic activity against two cancer cell lines, with potencies comparable to other reported combilexins, such that the hybrid agents are ~10−40-fold more toxic than either of the molecular components. Interestingly, this increased potency is in qualitative agreement with the improvement in DNA-binding affinity.

The comparative data (Tables 2 and 3) suggest that combilexins containing a proflavine rather than an acridine would result in (i) substantially greater DNA binding, (ii) markedly increased cytotoxicity, and (iii) improved aqueous solubility. Such replacement would alleviate the difficulties that arise due to poor protonation of the simpler acridine. Our modeling studies establish that acridine and, in particular, proflavine chromophores have a preferred orientation for DNA intercalation that favors delivery of a 9-aryl substituent into the minor groove. On this basis, we suggest that these hybrid molecules may be suitable for further elaboration as 'threading'-type combilexins, where the attached functions thread through the DNA helix and possibly lead to sequence-specific DNA recognition and improved antitumor potency.[30] Suitable attachment of secondary acridine substituents (e.g., by using an N10-alkylacridinium linkage) would facilitate unambiguous delivery of moieties directed toward simultaneous sensing of *both* the major and minor grooves. Synthesis of proflavine analogues based upon the prototype acridine derivatives is currently in progress.

Experimental Section

Synthetic Chemistry. The ^{1}H-NMR spectra were recorded at 250 MHz (300 K in DMSO-d_6, unless otherwise stated) with a Bruker AC250 spectrometer, using Me_4Si as internal standard. A Perkin-Elmer 1720X-FT instrument furnished the IR spectra. UV−visible spectra (EtOH) were obtained with a Shimadzu UV-2101PC instrument; ϵ values are given in units of M^{-1} cm^{-1}. Mass spectra (MS and high-resolution MS (HRMS)) were recorded with a VG-7070H spectrometer (source T = 115−150 °C) using either electron impact (EI: 70 V, 100 mA) or chemical ionization (CI: 50 eV, CH_4) techniques. Fast-atom bombardment (FAB: glycerol matrix) spectra were obtained using xenon (5 keV, 1 mA). Melting points (mp) were determined on a hot-stage apparatus and are uncorrected. Elemental analyses were carried out by Medac Ltd. (Brunel University, Uxbridge, U.K.); results for elements indicated by symbols are within ±0.4% of the theoretical values. TLC was carried out with silica gel (Merck 60F-254), with visualization at 254/366 nm and/or by I_2 staining, using the following eluent systems: A, $CHCl_3$−MeOH (98:2, v/v); B, $CHCl_3$−MeOH (95:5, v/v); C, $CHCl_3$−MeOH (90:10, v/v); and D, $CHCl_3$−MeOH (80:20, v/v). Column and radial chromatography were accomplished using silica gel (Merck 9385 or 15111 and Merck 7749, respectively) or alumina (neutral 90, Merck 1077). 9-Phenylacridine was prepared by a literature procedure.[19]

Proton NMR Assignments. Unambiguous NMR assignments for the acridine ring protons were established in $CDCl_3$ solution at 297 K by titration with the lanthanide shift reagent Eu(fod)$_3$ ('Resolve-Al EuFOD'). In each case, the rank order for perturbation of chemical shift is given by: H-4/5 ≫ H-9 > H-1/8 > H-3/6 ≈ H-2/7, with all protons resonating at lower chemical shift value. Assignments for the H-2/7 and H-3/6 protons (where present) were confirmed using spin decoupling and 2-D NOESY methods (results not shown).

5-[2-[(Tetrahydro-2*H*-pyran-2-yl)oxy]ethyl]-4-methylthiazole (2). A solution containing thiazole **1** (20.00 g, 0.14 mol), 3,4-dihydro-2*H*-pyran (DHP; 23.1 g, 0.27 mol), and 4-toluenesulfonic acid monohydrate (1.90 g, 0.01 mol) in CH_2Cl_2 (200 mL) was heated to gentle reflux. After 6 h, further DHP (9.2 g, 0.11 mol) was added and reflux was continued for 2.5 h. After digestion in EtOAc and filtration through a bed of alumina, solvent removal *in vacuo* afforded **2** (31.53 g, 99%) as a pale yellow oil: IR (film) 3074, 2943, 1723 (br), 1543, 1441, 1416, 1381, 1353 cm^{-1}; NMR ($CDCl_3$) δ 1.51–1.81 (m, 6H, $O(CH_2)_3$), 2.42 (s, 3H, thiazole-CH_3), 3.05 (t, J = 6.5 Hz, 2H, thiazole-CH_2CH_2), 3.45–3.60 (m, 2H, thiazole-CH_2CH_2), 3.70–3.75 (m, 1H, $O(CH)CH_aH_b$), 3.88–3.94 (m, 1H, $O(CH)CH_aH_b$), 4.62 (t, J = 3.2 Hz, 1H, $O(CH)O$), 8.57 (s, 1H, H-2); MS (CI: CH_4) m/z (rel intensity) 228 ($[M + H]^{+}$, 42), 144 ($[M - C_5H_7O]^{+}$, 48), 126 ($[M - C_5H_9O_2]^{+}$, 78), 125 (34), 112 (29), 101 (73), 100 (29), 99 (43), 85 ($[C_5H_9O]^{+}$, 100), 83 (51), 71 (37).

2-[2-(9-Acridinyl)-4-methyl-5-thiazolyl]ethanol (4). A solution of 1-butyllithium (1.6 M solution in hexanes, 96.0 mmol) was added dropwise to a stirred solution of **2** (20.00 g, 88.0 mmol) in anhydrous THF (30 mL) maintained beneath a blanket of N_2 at −78 °C. After 45 min, a solution of acridinone **3**[19] (22.4 g, 79.0 mmol) in anhydrous THF (80 mL) was added and the mixture was allowed to warm to room temperature. After 4 h, water was added and solvent removed *in vacuo*. The residue was digested in EtOH (75 mL) and aqueous HCl (2 M, 75 mL) and heated at 40 °C for 10 h. Neutralization with Na_2CO_3 gave a solid which was extracted with $CHCl_3$–MeOH (9:1, v/v, 400 mL). Recrystallization from MeCN afforded **4** (18.35 g, 73%) as a yellow crystalline solid: mp 173–175 °C; IR (KBr) 3305 (br, OH), 2867, 1519, 1436 cm^{-1}; NMR ($CDCl_3$) δ 2.55 (s, 3H, thiazole-CH_3), 3.12 (t, J = 6.4 Hz, 2H, CH_2CH_2-OH), 3.93 (t, J = 6.4 Hz, 2H, CH_2CH_2OH), 7.49 (AB_2M m, ^3J = 7.7 Hz, ^4J = 1.0 Hz, 2H, H-2/7), 7.77 (AB_2M m, ^3J = 7.7 Hz, ^4J = 1.1 Hz, 2H, H-3/6), 7.91 (br ABM m, ^3J = 7.7 Hz, 2H, H-1/8), 8.26 (ABM q, ^3J = 7.7 Hz, ^4J = 0.7 Hz, 2H, H-4/5); UV 384 (sh) (log ϵ 3.93), 362 (4.19), 346 (3.97), 253 (5.19), 216 (4.45) nm; MS (EI) m/z (rel intensity) 321 ($[M + H]^{+}$, 24), 320 ($[M]^{+}$, 100), 319 ($[M - H]^{+}$, 56), 289 ($[M - CH_2OH]^{+}$, 43), 85 (21); R_f 0.31 (solvent B). Anal. ($C_{19}H_{16}N_2OS$) C, H, N, S.

2-[2-(9-Acridinyl)-4-methyl-5-thiazolyl]ethyl 4′-Nitrobenzoate (5). 4-Nitrobenzoyl chloride (17.50 g, 94 mmol) was added with stirring to a refluxing solution of **4** (15.00 g, 47 mmol) in CH_2Cl_2 (200 mL) and pyridine (7 mL). After 10 h, further acid chloride (3.00 g, 16 mmol) was added and reflux continued for 2 h. On cooling, the solution was washed with dilute aqueous Na_2CO_3 and then water, and the organic phase was dried ($MgSO_4$), filtered, and concentrated. Trituration with Et_2O afforded **5** (20.00 g, 91%) as pale yellow needles: mp 189–190 °C; IR (KBr) 1733 (C=O), 1523 + 1348 (NO_2), 1270 cm^{-1}; NMR ($CDCl_3$) δ 2.63 (s, 3H, CH_3), 3.45 (t, J = 6.5 Hz, 2H, CH_2CH_2OCO), 4.71 (t, J = 6.5 Hz, 2H, CH_2CH_2OCO), 7.51 (br AB_2M m, ^3J = 7.7 Hz, 2H, H-2/7), 7.80 (AB_2M m, ^3J = 7.7 Hz, ^4J = 1.2 Hz, 2H, H-3/6), 7.89 (br ABM m, ^3J = 7.7 Hz, 2H, H-1/8), 8.22–8.30 (br m, 6H, H-4/5, H-2′/3′/5′/6′); UV 385 (sh) (log ϵ 3.85), 362 (4.11), 347 (sh) (3.91), 253 (5.14), 213 (4.47), 202 (4.48) nm; MS (CI: CH_4) m/z (rel intensity) 498 ($[M + C_2H_5]^{+}$, 16), 471 ($[M + 2H]^{+}$, 27), 470 ($[M + H]^{+}$, 93), 469 ($[M]^{+}$, 35), 440 (30), 303 ($[M - C_7H_4NO_4]^{+}$, 29), 302 ($[M - C_7H_5NO_4]^{+}$, 50), 59 (37), 57 (27); R_f 0.67 (solvent B). Anal. ($C_{26}H_{19}N_3O_4S$) C, H, N, S.

Synthesis of 2-[2-(9,10-Dihydroacridin-9-yl)-4-methyl-5-thiazolyl]ethyl 4′-Aminobenzoate (7) by Catalytic Hydrogenation of 5. A mixture of **5** (5.00 g, 10.65 mmol) and Pd–C catalyst (10%, w/w Pd, 0.50 g) was suspended in THF (100 mL) and hydrogenated using a Parr shaker apparatus (45 psi, room temperature) for 3 h. Removal of catalyst by filtration and solvent removal gave a solid that was digested in $CHCl_3$–MeOH (9:1, v/v). Trituration with hexane and filtration gave a bright yellow solid consistent with formulation as the acridan **7** (4.00 g, 85%): NMR ($CDCl_3$) δ 2.18 (s), 2.32 (s, 3H, CH_3), 3.00 (t, J = 6.7 Hz, 2H, CH_2CH_2O), 4.29 (t, J = 6.7 Hz, 2H, CH_2CH_2O), 5.71 (s, 1H, H-9), 6.26 (s, 1H, D_2O removes, 10-H), 6.77 (br ABM m, 2H, H-1/8), 6.86–6.93 (br AB_2M m, 2H, H-2/7), 6.94 (AB q, J = 8.7 Hz, 2H, H-3′/5′), 7.17 (br AB_2M m, 2H, H-3/6), 7.32 (br ABM m, 2H, H-4/5), 7.85 (AB q, J = 8.7 Hz, 2H, H-2′/6′); MS (FAB) m/z (rel intensity) 442 ($[M + H]^{+}$, 17), 441 ($[M]^{+}$, 57), 439 ($[M - 2H]^{+}$, 13); HRMS obsd 441.1524, calcd for $C_{26}H_{23}N_3O_2S$ 441.1511.

4-(2′,4′,6′-Trimethylbenzenesulfonamido)benzoic Acid (9). A solution of 2-mesitylenesulfonyl chloride (MtsCl; 31.95 g, 0.15 mol) in CH_2Cl_2 (100 mL) was added during 30 min to a solution of 4-aminobenzoic acid (**8**; 20.00 g, 0.15 mol) in pyridine (50 mL) and CH_2Cl_2 (50 mL). After reflux for 1.5 h, the mixture was cooled and concentrated *in vacuo*. Recrystallization from EtOH, with charcoal treatment, afforded sulfonamide **9** (29.38 g, 63%) as a colorless solid: mp 212.5–213 °C dec; IR (KBr) 3303 (NH), 3200, 2940, 1703 (C=O), 1610, 1516, 1406 cm^{-1}; NMR δ 2.22 (s, 3H, 4′-CH_3), 2.60 (s, 6H, 2′,6′-CH_3), 7.03 (s, 2H, H-3′/5′), 7.04 (AB m, J = 8.3, 1.2 Hz, 2H, H-3/5), 7.78 (AB m, J = 8.3, 1.2 Hz, 2H, H-2/6); MS (FAB) m/z (rel intensity) 320 ($[M + H]^{+}$, 30), 259 (24), 207 (31); R_f 0.29 (solvent C). Anal. ($C_{16}H_{17}NO_4S$) C, H, N, S.

2-[2-(9-Acridinyl)-4-methyl-5-thiazolyl]ethyl 4′-(2″,4″,6″-Trimethylbenzenesulfonamido)benzoate (10). A mixture of **4** (10.00 g, 31.21 mmol), sulfonamide **9** (20.00 g, 62.6 mmol), and 4-(dimethylamino)pyridine (3.80 g, 31.1 mmol) was suspended in anhydrous THF (300 mL) and stirred beneath a blanket of argon. 1,3-Dicyclohexylcarbodiimide (DCC; 12.90 g, 62.5 mmol) and oven-dried molecular sieves (3 g, type 4A) were added, and the mixture was stirred at room temperature for 21 h and then heated at 50 °C for 2 h. The cooled mixture was filtered and the filtrate washed serially with saturated aqueous K_2CO_3 solution, dilute aqueous AcOH, and water. The dried organic phase was concentrated and the residue digested in hot CH_2Cl_2, treated with decolorizing charcoal, and filtered while hot. Trituration with petroleum ether (bp 60–80 °C fraction) gave ester **10** (11.57 g, 60%) as a yellow crystalline solid: mp 210–214 °C; IR (KBr) 3262, 2930, 1696 (C=O), 1605, 1511, 1337 cm^{-1}; NMR δ 2.14 (s, 3H, 4″-CH_3), 2.51 (s, 3H, thiazole-CH_3), 2.55 (s, 6H, 2″,6″-CH_3), 3.37 (t, J = 5.9 Hz, 2H, CH_2CH_2OCO), 4.54 (t, J = 5.9 Hz, 2H, CH_2CH_2OCO), 6.94 (s, 2H, H-3″/5″), 7.03 (AB q, J = 8.6 Hz, 2H, H-3′/5′), 7.58 (br AB_2M m, ^3J = 7.7 Hz, 2H, H-2/7), 7.78 (br ABM m, ^3J = 7.7 Hz, 2H, H-1/8), 7.83 (AB q, J = 8.6 Hz, 2H, H-2′/6′), 7.90 (br AB_2M m, ^3J = 7.7 Hz, 2H, H-3/6), 8.26 (br ABM m, ^3J = 7.7 Hz, 2H, H-4/5); UV 386 (sh) (log ϵ 3.82), 362 (4.09), 345 (3.89), 278 (sh) (4.37), 253 (5.12), 205 (4.95) nm; MS (FAB) m/z (rel intensity) 623 ($[M + H]^{+}$, 46), 622 ($[M]^{+}$, 61), 532 (18), 439 ($[M - C_9H_{11}O_2S]^{+}$, 20), 391 (22), 303 ($[M - C_{16}H_{16}NO_4S]^{+}$, 98), 302 ($[M - C_{16}H_{17}NO_4S]^{+}$, 100), 301 ($[M - C_{16}H_{18}NO_4S]^{+}$, 54); R_f 0.47 (solvent B). Anal. ($C_{35}H_{31}N_3O_4S_2 \cdot H_2O$) C, H, N; S: calcd, 10.17; found, 9.13.

2-[2-(9-Acridinyl)-4-methyl-5-thiazolyl]ethyl 4′-Aminobenzoate (6). A solution of **10** (3.00 g, 4.83 mmol) in methanesulfonic acid (50 mL) was stirred at room temperature for 30 min, the reaction quenched with water, and the mixture adjusted to pH 9–10 using dilute aqueous KOH. The resulting brown solid was extracted with CH_2Cl_2–MeOH (9:1, v/v, 100 mL) and the organic phase washed with water, dried ($MgSO_4$), and concentrated. Recrystallization from MeCN gave **6** (1.96 g, 92%) as a yellow crystalline solid: mp 178–180 °C; IR (KBr) 3412 (NH), 3318, 3173, 1690 (C=O), 1650, 1602, 1519 cm^{-1}; NMR ($CDCl_3$) δ 2.62 (s, 3H, CH_3), 3.39 (t, J = 6.4 Hz, 2H, CH_2CH_2OCO), 4.08 (br s, D_2O removes, NH_2), 4.60 (t, J = 6.4 Hz, 2H, CH_2CH_2OCO), 6.63 (AB q, J = 8.7 Hz, 2H, H-3′/5′), 7.52 (AB_2M m, ^3J = 7.7 Hz, J = 1.1 Hz, 2H, H-2/7), 7.80 (AB_2M m, ^3J = 7.6 Hz, ^4J = 1.3 Hz, 2H, H-3/6), 7.88 (AB q, J = 8.7 Hz, 2H, H-2′/6′), 7.91 (br ABM m, ^3J = 7.7 Hz, 2H, H-1/8), 8.30 (br ABM m, ^3J = 7.6 Hz, 2H, H-4/5); UV 385 (sh) (log ϵ 3.94), 362 (4.20), 347 (3.99), 298 (4.47), 253 (5.23), 217 (4.60) nm; MS (EI) m/z (rel intensity) 439 ($[M]^{+}$, 7), 320 ($[M - C_7H_5NO]^{+}$, 83), 319 ($[M - C_7H_6NO]^{+}$, 45), 289 ($[M - C_8H_8NO_2]^{+}$, 46), 120 ($[C_7H_6NO]^{+}$, 16); R_f 0.39 (solvent B). Anal. ($C_{26}H_{21}N_3O_2S$) C, H, N, S.

General Alkylation Procedure. 2-(Dimethylamino)ethyl 4-Aminobenzoate (14). A suspension of 4-aminobenzoic acid (**8**; 47.60 g, 0.35 mol), 2-chloro-*N*,*N*-dimethylethylamine hydrochloride (50.00 g, 0.35 mol), and anhydrous $NaHCO_3$ (120 g, 1.43 mol) in acetone (500 mL) was stirred

with gentle reflux. After 6 h, the mixture was cooled using an external ice–water bath and filtered. Solvent removal afforded a pale yellow oil which was dissolved in CH_2Cl_2 (200 mL) and washed with saturated Na_2CO_3 (2 × 150 mL aliquots) and water (100 mL). The organic solution was dried (Na_2SO_4) and concentrated under reduced pressure to give a colorless oil which crystallized spontaneously. The product was dissolved in hot EtOAc, boiled with decolorizing charcoal, and filtered. On cooling the title ester **14** (54.13 g, 75%) appeared as colorless prismatic needles: mp 120–121 °C; IR (KBr) 3434 (NH), 3334, 3188, 2823, 2773, 1678 (C=O), 1600 cm^{-1}; NMR ($CDCl_3$) δ 2.33 (s, 6H, NCH_3), 2.69 (t, J = 5.8 Hz, 2H, $CH_2CH_2N(CH_3)_2$), 4.12 (br s, 2H, D_2O exchanges, NH_2), 4.37 (t, J = 5.8 Hz, 2H, $CH_2CH_2N(CH_3)_2$), 6.63 (AB q, J = 8.6 Hz, 2H, H-3/5), 7.85 (AB q, J = 8.6 Hz, 2H, H-2/6); MS (EI) m/z (rel intensity) 209 ($[M + H]^{\bullet+}$, 9%), 164 ($[M - NMe_2]^{\bullet+}$, 3), 120 ($[M - C_4H_{10}NO]^{\bullet+}$, 35), 92 ($[M - C_5H_{10}NO_2]^{\bullet+}$, 13), 71 ($[C_4H_9N]^{\bullet+}$, 100), 58 ($[C_3H_8N]^{\bullet+}$, 100); R_f 0.25 (solvent C). Anal. ($C_{11}H_{16}N_2O_2$) C, H, N.

General Diazotization–Coupling Procedure. 2-[2-(9-Acridinyl)-4-methyl-5-thiazolyl]ethyl 4′-[1*H*-[4″-[[2-(Dimethylamino)ethoxy]carbonyl]phenyl]-3-triazeno]benzoate (22). Amine **6** (500 mg, 1.14 mmol) was suspended in 2 M aqueous HCl (6 mL) and DMSO (1 mL) and cooled to 0–5 °C using an external ice–water bath. A solution of $NaNO_2$ (79 mg, 1.14 mmol) in water (3 mL) was then introduced dropwise with stirring, and the mixture was stirred at this temperature for 1 h. A solution of aniline **14** (237 mg, 1.14 mmol) in 2 M aqueous HCl (3 mL) was added and the stirred mixture adjusted to pH 6 by addition of solid NaOAc. After stirring for 1 h, the mixture was adjusted to pH 7 using solid NaOAc. The product was extracted with $CHCl_3$–MeOH (9:1, v/v), and the organic phase was dried ($MgSO_4$), filtered, and concentrated under reduced pressure to give a yellow/orange solid. Radial chromatography (silica gel, 5%, v/v, MeOH–$CHCl_3$) afforded **22** (0.46 g, 62%) as a yellow powder: mp 153–155 °C dec; IR (KBr) 2959 (br), 1722 (br) (C=O), 1606, 1524 cm^{-1}; NMR ($CDCl_3$) δ 2.36 (s, 6H, NCH_3), 2.64 (s, 3H, CH_3), 2.75 (t, J = 5.8 Hz, 2H, $CH_2CH_2N(CH_3)_2$), 3.43 (t, J = 6.3 Hz, 2H, CH_2CH_2OCOAr), 4.45 (t, J = 5.8 Hz, 2H, $CH_2CH_2N(CH_3)_2$), 4.67 (t, J = 6.3 Hz, 2H, CH_2CH_2OCOAr), 7.44 (AB q, J = 8.7 Hz, 2H, H-2″/6″, established by spin decoupling), 7.45 (AB q, J = 8.7 Hz, 2H, H-3′/5′), 7.47–7.54 (br AB_2M m, 2H, H-2/7), 7.79 (br AB_2M m, ^3J = 7.5 Hz, 2H, H-3/6), 7.91 (br ABM m, 2H, H-1/8), 8.06 (AB q, J = 8.6 Hz, 2H, H-2′/6′), 8.11 (AB q, J = 8.5 Hz, 2H, H-3″/5″), 8.27 (br ABM m, ^3J = 7.5 Hz, 2H, H-4/5); UV 370 (sh), (log ϵ 4.69), 364 (4.70), 253 (5.19), 214 (4.57) nm; MS (FAB) m/z (rel intensity) 659 ($[M]^{\bullet+}$, 15%), 302 ($[M - C_{18}H_{20}N_4O_4]^{\bullet+}$, 32); R_f 0.40 (solvent C). Anal. ($C_{37}H_{34}N_6O_4S{\cdot}H_2O$) C, H, N, S.

2-[2-(9-Acridinyl)-4-methyl-5-thiazolyl]ethyl 4′-[1*H*-(4″-Amidinophenyl)-3-triazeno]benzoate (18). Aniline **6** (500 mg, 1.14 mmol) was diazotized and treated with a solution of 4-aminobenzamidine dihydrochloride (0.24 g, 1.14 mmol) using the general procedure. After stirring for 18 h at room temperature, the crude product was collected by filtration and washed with water. Digestion in MeOH–$CHCl_3$ (50%, v/v) and trituration with petroleum ether (bp 60–80 °C fraction) gave **18** (0.36 g, 54%) as a yellow/orange solid: mp 192–194 °C dec; NMR δ 2.56 (s, 3H, CH_3), 3.46 (br t, 2H, CH_2CH_2O), 4.63 (t, J = 5.7 Hz, 2H, CH_2CH_2O), 7.56–7.65 (br m, 6H, H-2/7, H-3′/5′, H-2″/6″), 7.81–7.93 (br m, 6H, H-3/6, H-1/8, H-3″/5″), 8.03 (AB q, J = 8.6 Hz, 2H, H-2′/6′), 8.26 (br ABM m, 2H, H-4/5); MS (FAB) m/z (rel intensity) 586 ($[M]^{\bullet+}$, 22), 429 (31), 306 (100), 303 ($[M - C_{14}H_{12}N_5O_2]^{\bullet+}$, 36); HRMS obsd 586.2035, calcd for $C_{33}H_{28}N_7O_2S$ 586.2025.

3,6-Diamino-9(10*H*)-acridinone (24). A mixture of concentrated aqueous HCl (300 mL) and anhydrous tin(II) chloride (94.80 g, 0.50 mol) was heated to reflux (CARE! HCl gas evolved). 2,2′,4,4′-Tetranitrobenzophenone[31] (15.0 g, 41.41 mmol) was then added during 15 min while maintaining the mixture at 90–100 °C. Concentrated aqueous HCl (30 mL) and EtOH (25 mL) were then added, and reflux was continued for 3 h. On cooling, further concentrated aqueous HCl (50 mL) was added and the mixture left to stand for 18 h. The precipitate was collected by filtration and partially dried in air, digested in hot aqueous HCl (0.1 M, 230 mL), boiled with decolorizing charcoal, and filtered. On cooling, the filtrate was adjusted to pH 13 with aqueous NaOH, heated to reflux for 20 min to dissolve any inorganic materials, and filtered. The solid was washed with aqueous NaOH (20%, w/w, 50 mL) followed by hot water and dried *in vacuo* (P_2O_5) to furnish acridinone **24** (5.83 g, 62%). Radial chromatography (silica gel, 20%, v/v, MeOH–$CHCl_3$) provided an analytical sample as a cream-colored solid: mp >300 °C (lit.[20] mp >320 °C); IR (KBr) 3337 + 3214 (NH), 1637, 1595, 1526, 1473 cm^{-1}; NMR δ 5.86 (br s, 4H, D_2O exchanges, NH_2), 6.32 (d, ^4J = 1.9 Hz, 2H, H-4/5), 6.39 (dd, ^3J = 8.7 Hz, ^4J = 1.9 Hz, 2H, H-2/7), 7.77 (d, ^3J = 8.7 Hz, 2H, H-1/8), 10.57 (br s, 1H, D_2O exchanges, H-10); UV 360 (log ϵ 4.45), 306 (3.66), 268 (4.92), 234 (4.28) nm; MS (EI) m/z (rel intensity) 446 (13), 225 ($[M]^{\bullet+}$, 100), 91 (65); R_f 0.33 (solvent D). Anal. ($C_{13}H_{11}N_3O{\cdot}0.1H_2O$) C, H, N.

3,6-Bis[(ethoxycarbonyl)amino]-9(10*H*)-acridinone (25). Ethyl chloroformate (8.51 g, 78.4 mmol) was added dropwise to a stirred solution of acridinone **24** (3.50, 15.5 mmol) in *N*,*N*-diethylaniline (14 mL) and the mixture heated to 90 °C for 30 min. On cooling, MeOH (50 mL) and 2 M aqueous HCl (50 mL) were added, and the volatiles were removed by boiling. The resulting brown precipitate was filtered, washed with 2 M aqueous HCl and water, and dried *in vacuo* (P_2O_5, <0.5 mbar). The product was digested in hot EtOH, treated with decolorizing charcoal, filtered, and triturated with water. Filtration and recrystallization from DMF–water (4:1, w/v) gave carbamate **25** (2.30 g, 40%) as a light-brown solid: mp >250 °C dec (lit.[20] mp 270 °C); NMR δ 1.28 (t, J = 7.1 Hz, 6H, CH_3), 4.19 (q, J = 7.1 Hz, 4H, CH_2), 7.17 (dd, ^3J = 8.8 Hz, ^4J = 1.9 Hz, 2H, H-2/7), 7.85 (d, ^4J = 1.8 Hz, 2H, H-4/5), 8.05 (d, ^3J = 8.8 Hz, 2H, H-1/8), UV 384 (log ϵ 4.04), 366 (4.06), 333 (4.45), 277 (5.13), 230 (4.54) nm; MS (FAB) m/z (rel intensity) 371 ($[M + 2H]^{\bullet+}$, 28%), 370 ($[M + H]^{\bullet+}$, 91), 369 ($[M]^{\bullet+}$, 17), 342 (6), 324 ($[M - C_2H_5O]^{\bullet+}$, 6), 297 (8), 252 (9), 207 (11). Anal. ($C_{19}H_{19}N_3O_5{\cdot}0.5H_2O$) C, H, N.

3,6-Bis[[(2-methoxyethoxy)methyl](ethoxycarbonyl)amino]-10-[(2-methoxyethoxy)methyl]-9(10*H*)-acridinone (26). A solution of **25** (1.00 g, 2.71 mmol) in anhydrous THF (20 mL) was treated with NaH (80%, w/w, dispersion in oil, 0.41 g, 13.67 mmol) and stirred for 40 min. The mixture was cooled to 0–5 °C, treated with MEM chloride (1.69 g, 13.58 mmol), and allowed to warm to room temperature. After 1 h, the reaction was quenched cautiously with water and the mixture concentrated and extracted with EtOAc and dilute aqueous K_2CO_3–NaCl solution. The organic phase was separated, washed with water, dried (Na_2SO_4), and concentrated. Purification by chromatography (silica gel, solvent system B) afforded acridinone **26** (0.91 g, 53%) as a brown oil: NMR ($CDCl_3$) δ 1.28 (t, J = 7.1 Hz, 6H, OCH_2CH_3), 3.39–3.40 (m, OCH_3), 3.54–3.88 (m, 4H, $CH_2CH_2OCH_3$), 4.25 (q, J = 7.1 Hz, 4H, OCH_2CH_3), 4.83 (s, unassigned MEM-CH_2), 5.23 (s, 4H, NCH_2O), 5.76 (s, 2H, N(10)-CH_2O), 7.30 (dd, ^3J = 8.7 Hz, ^4J = 1.8 Hz, 2H, H-2/7), 7.79 (d, ^4J = 1.7 Hz, 2H, H-4/5), 8.47 (d, ^3J = 8.6 Hz, 2H, H-1/8); MS (FAB) m/z (rel intensity) 635 ($[M + H]^{\bullet+}$, 39%), 634 ($[M]^{\bullet+}$, 100). This material (85–90% by NMR) was used without further purification.

9-Phenyl-3,6-bis[(ethoxycarbonyl)amino]acridine (27). A solution of PhMgCl (2 M solution in Et_2O, 0.80 mmol) was added to a stirred solution of **26** (0.45 g, 0.71 mmol) in dry THF (5 mL) at −78 °C. Three further portions of PhMgCl solution (0.40 mmol) were introduced during 18 h stirring at room temperature. The reaction was quenched with water and the mixture concentrated, treated with 2 M aqueous HCl (10 mL) and EtOH (10 mL), and heated to 60 °C for 30 min. Concentrated aqueous HCl (5 mL) was added and heating continued for 1 h. After stirring for 15 h at room temperature, the mixture was neutralized (K_2CO_3) and extracted with EtOAc. The organic phase was washed with water, dried ($MgSO_4$), filtered, and concentrated. Radial chromatography (silica gel, solvent system C) gave **27** (0.13 g, 42%) as a bright

yellow powder: mp >150 °C dec; IR (KBr) 2978 (br), 1736, 1632, 1610, 1553, 1459, 1200 cm^{-1}; NMR δ 1.29 (t, J = 7.1 Hz, 6H, CH_2CH_3), 4.21 (q, J = 7.1 Hz, 4H, CH_2CH_3), 7.44–7.54 (br m, 6H, H-1/8, H-2/7, H-2′/6′), 7.63–7.65 (br m, 3H, H-3′/4′/5′), 8.29 (d, J = 1.7 Hz, 2H, H-4/5); UV 421 (log ϵ 4.35), 391 (4.27), 274 (4.99), 241 (4.44) nm; MS (FAB) m/z (rel intensity) 431 ($[M + 2H]^{\cdot+}$, 31), 430 ($[M + H]^{\cdot+}$, 100), 185 (24), 93 (90), 89 (24), 57 (34); R_f 0.60 (solvent C). Anal. ($C_{25}H_{23}N_3O_4 \cdot 0.25H_2O$), C, H, N.

9-Phenyl-3,6-diaminoacridine (28). A stirred mixture of **27** (50.0 mg, 0.12 mmol) and aqueous HBr (10 mL of 48%, w/w, solution) was refluxed for 2 h. On cooling, the mixture was adjusted to pH 9 with solid K_2CO_3 and extracted with MeOH–$CHCl_3$ (1:4, v/v). The organic solution was dried ($MgSO_4$), filtered, and concentrated and the residue digested in MeOH and then treated with excess ethereal HCl. The formed precipitate was collected, washed with ethereal HCl followed by Et_2O, and dried in air to give the hydrochloride salt of **28** (23.5 mg, 61%) as a red powder: IR (KBr) 3307 + 3182 (br) (NH), 1626, 1474 cm^{-1}; NMR δ 6.78–6.82 (br m, 4H, H-2/7, H-4/5), 7.14 (d, ^3J = 9.0 Hz, 2H, H-1/8), 7.36–7.39 (br m, 2H, H-2′/6′), 7.60–7.62 (br m, 3H, H-3′/4′/5′); UV 465 (log ϵ 4.46), 3.16 (sh) (3.68), 265 (4.61), 286 (4.33) nm; MS (FAB) m/z (rel intensity) 287 ($[M + 2H]^{\cdot+}$, 8), 286 ($[M + H]^{\cdot+}$, 28); HRMS obsd 286.1355, calcd for $C_{19}H_{16}N_3$ 286.1344 ($[M + H]^{\cdot+}$).

Thermal Denaturation Studies. Optical thermal denaturation experiments were performed in stoppered quartz cuvettes using a Varian-Cary 219 spectrophotometer fitted with a Neslab ETP-3/RTE4 circulating heating/cooling thermoprogrammer, as detailed previously.[32] Heating was applied at 1 °C/min until denaturation was complete, as judged from the increase in optical absorbance at 260 nm. Calf thymus (CT-DNA) (type-I, highly polymerized sodium salt; 42% G + C content] and the synthetic oligonucleotides [poly(dA–dT)]$_2$ and [poly(dG–dC)]$_2$, both as sodium salts, were purchased from Sigma Chemical Co. Ltd. and used without further purification. Molar extinction values of ϵ_{260} = 6600, 6550, and 8400 (M phosphate)$^{-1}$ cm^{-1}, respectively, were used.[33] Aqueous solutions of the DNA samples were prepared in Millipore-purified water containing 10 mM sodium phosphate and 1 mM EDTA. Solutions were buffered at pH 7.00 ± 0.01 or 6.00 ± 0.01 for CT-DNA and at pH 6.00 ± 0.01 for the oligonucleotides; working solutions (100 μM) were prepared by dilution of a stock solution. DNA–drug solutions were prepared by addition of the ligand compound in DMSO to give a final drug concentration of 20 μM. A fixed drug:DNAp molar ratio of 1:5 was used throughout as this ratio was established to represent incomplete saturation of each DNA by the ligands under investigation.

In all DNA–drug studies, DMSO (max 6.25%, v/v) was used as cosolute to prevent precipitation of the ligands. Linear correction factors were applied to correct for the effects of DMSO in all working solutions. Thermal denaturation temperatures (T_m) for the DNA and DNA–ligand complexes were determined using a published procedure.[32] Values of 40.9 ± 0.1 and 94.2 ± 0.1 °C at pH 6 were established for [poly(dA–dT)]$_2$ and [poly(dG–dC)]$_2$, respectively. Similarly, CT-DNA gave T_m values of 63.7 ± 0.1 °C (pH 6) and 67.8 ± 0.1 °C (pH 7). The change in DNA-melting behavior (ΔT_m) induced by the added compound is given by $\Delta T_m = T_m$(DNA + ligand) – T_m(DNA), where T_m(DNA) represents the drug-free control. All induced shifts are reported as the mean from three determinations.

Fluorescence Binding Studies. The Q values for quenching were determined for each DNA (20 μM) in 0.01 M ionic strength aqueous buffer (9.3 mM NaCl, 2 mM NaOAc, 0.1 mM EDTA, pH 5.0) containing 2 μM ethidium bromide (Sigma), as described previously.[14a] These concentrations were selected to effect minimal ethidium displacement and maximum drug-induced quenching of fluorescence.[22] The CC_{50} values for ethidium displacement were determined using solutions in the same buffer containing 1.26 μM ethidium bromide and 1 μM CT-DNA.[14a,22,23] All measurements were made in 10-mm pathlength quartz cuvettes (3 mL) at 20 °C using a Perkin-Elmer LS5 spectrofluorometer (excitation at 546 nm; emission at 595 nm) following serial addition of aliquots of a stock drug solution (~5 mM in DMSO). The Q and CC_{50} values are defined as the drug concentrations which reduce the fluorescence of initially DNA-bound ethidium by 50%. Values are reported as the mean from three determinations. Apparent equilibrium binding constants (K_{app}) were calculated using a value of 10^7 M^{-1} for ethidum.[22a] Most compounds and their DNA-bound complexes showed neither optical absorption nor fluorescence at 595 nm and did not interfere with the fluorescence of unbound ethidium. However, these effects prevented determination of reliable competitive CC_{50} values for both proflavine and **28**.

***In Vitro* Cytotoxicity. A2780 Experimental Protocol.** The A2780 cells were grown in Dulbecco's modified medium containing 10% fetal calf serum, gentamicin (50 mg/mL), amphotericin B (2.5 mg/mL), glutamine (2 mM), insulin (10 mg/mL), and hydrocortisone (0.5 mg/mL). Single cells, harvested by trypsinization (0.02% EDTA/0.05% trypsin), were plated at (0.1–5) × 10^3 in 96-well microtiter plates and allowed to attach overnight. Compounds were dissolved in DMSO and diluted with buffer (pH 7.0) to give stock solutions containing ≤0.5%, v/v, DMSO. Drugs were added to the cells at various concentrations following dilution of the stock solution. After continuous exposure to the drug for 96 h, the cytotoxicity was assessed by staining with sulforhodamine B (SRB) as follows. The medium was aspirated, and the cells were exposed to ice-cold trichloroacetic acid (10%, w/v) for 30 min. The cells were then washed five times with water, held in SRB (100 mL of 0.4% solution in 1%, v/v, aqueous acetic acid) for 10–15 min, and then washed five times with 1% aqueous acetic acid. After air-drying overnight, the protein-bound SRB was solubilized with Tris base (100 mL of 10 mL) and the plates were assessed at 540 nm using a plate reader (Titertek Multiscan MCC/340, Flow Laboratories). By comparing treated with untreated control wells, IC_{50} values (concentration of drug required to inhibit the growth of cells by 50% when compared to solvent-treated but drug-free controls) were determined using a computer software package (Titersoft II, Flow Laboratories).

L1210 Experimental Protocol. Drug solutions of appropriate concentration were added to a cell culture containing mouse L1210 leukemic cells at 5 × 10^3 cells/mL of medium. Stock drug solutions containing ≤0.5%, v/v, DMSO were used, and it was separately established that this level of cosolvent was tolerated. Cells were exposed to the drugs for 48 h at 37 °C, and the IC_{50} values were calculated by counting the number of remaining living cells with a Coulter counter and comparison with drug-free controls. Assays were performed in duplicate.

Molecular Modeling and Energy Calculations. Models for the ligand molecules were generated using crystallographic bond lengths and angles.[34] The DNA sequence used for modeling was the d(GATAC·GATAC)·d(GTATC·GTATC) duplex, where the central 5′-CpG intercalation site is flanked on each side by a 3-bp AT tract, representing the 10-bp core of a dodecamer duplex used in an extended study of DNA intercalation by proflavine.[28]

Initial docked models were generated by graphics overlay of atomic coordinates for the acridine chromophore of each ligand with that of proflavine in the minimized DNA–proflavine complex.[28] Subsequent maneuvers involved graphics manipulation of the substituents and side chains to (i) remove unfavorable intermolecular atomic clash and (ii) locate groove-binding or interacting molecular fragments in their most favorable groove positions. Models for the intercalated complexes were examined for each possible ligand alignment, with the acridine N10 atom positioned in either the major or minor groove and any 9-substituent positioned in the corresponding minor or major groove. This situation is more complex for ligands bearing asymmetric 9-substituents as two distinct orientations of the attached function are possible, differing in the groove alignment of the polar residue with respect to the 5′ → 3′ direction of the d(GATACGATAC)

strand. Docked complexes were subjected to molecular mechanics (MM) energy minimization using the X-PLOR 3.1 package; the protocol used for minimization is described elsewhere.[7b] No advantage was discerned using a more rigorous molecular dynamics (MD) strategy, with a four-step MM–MD–MD–MM protocol resulting in qualitatively similar structures following simulation for either 20 or 50 ps at 300 K (not shown). Atom-centered molecular electrostatic potentials (MEPs) were used for all ligands and DNA nucleotides.[35] Necessary additional force field parameters were interpolated from earlier reports from this laboratory.[7a,b,8,10] Binding energies for interaction (Table 3) were calculated using $E_{bind} = E_{complex} - (E_{DNA} + E_{ligand})$, where the E_{DNA} and E_{ligand} terms represent the energies computed for the separately minimized free molecules. All DNA–ligand complexes were examined as the N10-protonated acridinium salts, although equivalent neutral, unprotonated forms were also studied for selected acridines. In the case of hybrid molecules **18–23**, the distal basic residues were examined as both the neutral and protonated species.

Acknowledgment. This work was supported by the Cancer Research Campaign and by a studentship from the Northern Ireland Education Department (to A.W.M.). We thank Stephen Neidle for his encouragement and Dr. P. Herzyk for providing DNA coordinates. We are grateful to Anthony Reszka for excellent technical assistance and both Dr. L. R. Kelland and the late George Abel (CRC Centre for Cancer Therapeutics) for providing cytotoxicity data.

References

(1) (a) Nielsen, P. E. Sequence-Selective DNA Recognition by Synthetic Ligands. *Bioconjugate Chem.* **1991**, *2*, 1–12. (b) Hurley, L. H., Ed. *Advances in DNA Sequence-Specific Agents*; JAI Press Inc.: Greenwich, CT, 1992.

(2) (a) Steitz, T. A. Structural Studies of Protein-Nucleic Acid Interaction: The Sources of Sequence-Specific Binding. *Q. Rev. Biophys.* **1990**, *23*, 205–280. (b) Freemont, P. S.; Lane, A. N.; Sanderson, M. R. Structural Aspects of Protein-DNA Recognition. *Biochem. J.* **1991**, *278*, 1–23.

(3) Crooke, S. T., Lebleu, B., Eds. *Antisense Research and Applications*; CRC Press: Boca Raton, FL, 1993.

(4) (a) Dervan, P. B. Design of Sequence-Specific DNA-Binding Molecules. *Science* **1986**, *232*, 464–471. (b) Zimmer, C.; Wähnert, U. Non-Intercalating DNA-Binding Ligands: Specificity of the Interaction and Their Use as Tools in Biophysical, Biochemical and Biological Investigations of the Genetic Material. *Prog. Biophys. Mol. Biol.* **1986**, *47*, 31–112.

(5) (a) Kopka, M. L.; Yoon, C.; Goodsell, D.; Pjura, P.; Dickerson, R. E. The Molecular Origin of DNA-Drug Specificity in Netropsin and Distamycin. *Proc. Natl. Acad. Sci. U.S.A.* **1985**, *82*, 1376–1380. (b) Coll, M.; Frederick, C. A.; Wang, A. H.-J.; Rich, A. A Bifurcated Hydrogen-Bonded Conformation in the d(A·T) Base-Pairs of the DNA Dodecamer d(CGCAAATTTGCG) and its Complex with Distamycin. *Proc. Natl. Acad. Sci. U.S.A.* **1987**, *84*, 8385–8389. (c) Lown, J. W. Lexitropsins: Rational Design of DNA Sequence Reading Agents as Novel Anti-Cancer Agents and Potential Cellular Probes. *Anti-Cancer Drug Des.* **1988**, *3*, 25–40.

(6) (a) Searle, M. S. NMR Studies of Drug-DNA Interactions. *Progr. NMR Spectrosc.* **1993**, *25*, 403–480. (b) Krugh, T. R. Drug-DNA Interactions. *Curr. Opin. Struct. Biol.* **1994**, *4*, 351–364 and references therein.

(7) (a) Lane, A. N.; Jenkins, T. C.; Brown, T.; Neidle, S. Interaction of Berenil with the *Eco*RI Dodecamer d(CGCGAATTCGCG)$_2$ in Solution studied by NMR. *Biochemistry* **1991**, *30*, 1372–1385. (c) Jenkins, T. C.; Lane, A. N.; Neidle, S.; Brown, D. G. NMR and Molecular Modeling Studies of the Interaction of Berenil and Pentamidine with d(CGCAAATTTGCG)$_2$. *Eur. J. Biochem.* **1993**, *213*, 1175–1184. (c) Yoshida, M.; Banville, D. L.; Shafer, R. H. Structural Analysis of d(GCAATTGC)$_2$ and Its Complex with Berenil by Nuclear Magnetic Resonance Spectroscopy. *Biochemistry* **1990**, *29*, 6585–6592.

(8) (a) Brown, D. G.; Sanderson, M. R.; Skelly, J. V.; Jenkins, T. C.; Brown, T.; Garman, E.; Stuart, D. I.; Neidle, S. Crystal Structure of a Berenil-Oligonucleotide Complex: The Role of Water in Sequence-Specific Ligand Binding. *EMBO J.* **1990**, *9*, 1329–1334. (b) Brown, D. G.; Sanderson, M. R.; Garman, E.; Neidle, S. Crystal Structure of a Berenil-d(CGCAAATTTGCG) Complex. An Example of Drug-DNA Recognition Based on Sequence-Dependent Structural Features. *J. Mol. Biol.* **1992**, *226*, 481–490.

(9) (a) Quintana, J. R.; Lipanov, A. A.; Dickerson, R. E. Low-Temperature Crystallographic Analysis of the Binding of Hoechst 33258 to the Double-Helical DNA Dodecamer CGCGAATTCGCG. *Biochemistry* **1991**, *30*, 10294–10306. (b) Nunn, C. M.; Jenkins, T. C.; Neidle, S. Crystal Structure of d(CGCGAATTCGCG) Complexed with Propamidine, a Short-Chain Homologue of the Drug Pentamidine. *Biochemistry* **1993**, *32*, 13838–13843.

(10) (a) Laughton, C. A.; Jenkins, T. C.; Fox, K. R.; Neidle, S. Interaction of Berenil with the *tyr*T DNA Sequence Studied by Footprinting and Molecular Modeling. Implications for the Design of Sequence-Specific DNA Recognition Agents. *Nucleic Acids Res.* **1990**, *18*, 4479–4488. (b) Greenidge, P. A.; Laughton, C. A.; Jenkins, T. C.; Neidle, S. Factors Involved in Guanosine/Cytosine (G/C) Selectivity of DNA-Binding Drugs: A Molecular Modeling Study of Ligand Interactions with a *tyr*T DNA Sequence. *J. Chem. Soc., Faraday Trans.* **1993**, *89*, 2651–2657. (c) Conte, M. R.; Jenkins, T. C.; Lane, A. N. Interaction of Minor Groove-Binding Diamidine Ligands with an Asymmetric DNA Duplex: NMR and Molecular Modelling Studies. *Eur. J. Biochem.* **1995**, *229*, 433–444.

(11) Bailly, C.; Hénichart, J.-P. Molecular Pharmacology of Intercalator-Groove Binder Hybrid Molecules. In *Molecular Aspects of Anticancer Drug-DNA Interactions*; Neidle, S., Waring, M., Eds.; Macmillan Press Ltd.: London, U.K., 1994; Vol. 2, pp 162–196.

(12) Krivtsova, M. A.; Moroshkina, E. B.; Glibin, E. DNA Interaction with Low Molecular Weight Ligands with Different Structures. III. Complexes of DNA with Distaxins. *Mol. Biol.* **1984**, *18*, 950–956.

(13) Eliadis, A.; Phillips, D. R.; Reiss, J. A.; Skorobogaty, A. The Synthesis and DNA Footprinting of Acridine-Linked Netropsin and Distamycin Bifunctional Mixed Ligands. *J. Chem. Soc., Chem. Commun.* **1988**, 1049–1052.

(14) (a) Bailly, C.; Pommery, N.; Houssin, R.; Hénichart, J.-P. Design, Synthesis, DNA Binding, and Biological Activity of a Series of DNA Minor Groove-Binding Intercalating Drugs. *J. Pharm. Sci.* **1989**, *78*, 910–917. (b) Bailly, C.; Helbecque, N.; Hénichart, J.-P.; Colson, P.; Houssier, C.; Rao, K. E.; Shea, R. G.; Lown, J. W. Molecular Recognition Between Oligopeptides and Nucleic Acids: DNA Sequence Specificity and Binding Properties of an Acridine-Linked Netropsin Hybrid Ligand. *J. Mol. Recognit.* **1990**, *3*, 26–35. (c) Bailly, F.; Baillÿ, C.; Helbecque, N.; Pommery, N.; Colson, P.; Houssier, C.; Hénichart, J.-P. Relationship Between DNA-Binding and Biological Activity of Anilinoacridine Derivatives Containing the Nucleic Acid-Binding Unit SPKK. *Anti-Cancer Drug Des.* **1992**, *7*, 83–100.

(15) Bourdouxhe, C.; Colson, P.; Houssier, C.; Sun, J.-S.; Montenay-Garestier, T.; Hélène, C.; Rivalle, C.; Bisagni, E.; Waring, M. J.; Hénichart, J.-P.; Bailly, C. Binding of a Distamycin-Ellipticene Hybrid Molecule to DNA and Chromatin: Spectroscopic, Biochemical, and Molecular Modeling Investigations. *Biochemistry* **1992**, *31*, 12385–12396.

(16) Subra, F.; Carteau, S.; Pager, J.; Paoletti, J.; Auclair, C.; Mrani, D.; Gosselin, G.; Imbach, J. L. Bis(pyrrolecarboxamide) Linked to Intercalating Chromophore Oxazolopyridocarbazole (OPC): Selective Binding to DNA and Polynucleotides. *Biochemistry* **1991**, *30*, 1642–1650.

(17) Shapiro, T. A.; Englund, P. T. Selective Cleavage of Kinetoplast DNA Minicircles Promoted by Antitrypanosomal Drugs. *Proc. Natl. Acad. Sci. U.S.A.* **1990**, *87*, 950–954.

(18) Goodsell, D.; Dickerson, R. E. Isohelical Analysis of DNA Groove-Binding Drugs. *J. Med. Chem.* **1986**, *29*, 727–733.

(19) 10-Alkylacridinone (**3**) was prepared by alkylation of 9(10*H*)-acridinone as per footnote 8 in: Zeng, Z.; Zimmerman, S. C. Convenient Synthesis of 9-Alkyl- and 9-Arylacridines from [2-(Trimethylsilyl)ethoxy]methyl (SEM) Protected Acridone. *Tetrahedron Lett.* **1988**, *29*, 5123–5124.

(20) Müller, W.; Gaedtke, H.; Conradt, P. Preparation and Properties of Some Biologically Interesting Acridine Dyes. *Liebigs Ann. Chem.* **1973**, 993–1003.

(21) Baguley, B. C. Nonintercalative DNA-Binding Antitumour Compounds. *Mol. Cell Biochem.* **1982**, *43*, 167–181.

(22) (a) Morgan, A. R.; Lee, J. S.; Pulleyblank, D. E.; Murray, N. L.; Evans, D. H. Review: Ethidium Fluorescence Assays. Part 1. Physicochemical Studies. *Nucleic Acids Res.* **1979**, *7*, 547–569. (b) Baguley, B. C.; Denny, W. A.; Atwell, G. J.; Cain, B. F. Potential Antitumor Agents. 34. Quantitative Relationships between DNA Binding and Molecular Structure for 9-Anilinoacridines Substituted in the Anilino Ring. *J. Med. Chem.* **1981**, *24*, 170–177.

(23) Jenkins, T. C.; Parrick, J.; Porssa, M. DNA-Binding Properties of Nitroarene Oligopeptides Designed as Hypoxia-Selective Agents. *Anti-Cancer Drug Des.* **1994**, *9*, 477–493.

(24) Feigon, J.; Denny, W. A.; Leupin, W.; Kearns, D. R. Interactions of Antitumor Drugs with Natural DNA: ^{1}H-NMR Study of Binding Mode and Kinetics. *J. Med. Chem.* **1984**, *27*, 450–465.

(25) (a) Bailly, C.; Helbecque, N.; Hénichart, J.-P.; Colson, P.; Houssier, C.; Rao, K. E.; Shea, R. G.; Lown, J. W. Molecular Recognition between Oligopeptides and Nucleic Acids. DNA

Sequence Specificity and Binding Properties of an Acridine-Linked Netropsin Hybrid Ligand. *J. Mol. Recognit.* **1990**, *3*, 26–35. (b) Bourdouxhe, C.; Colson, P.; Houssier, C.; Hénichart, J.-P.; Waring, M. J.; Denny, W. A.; Bailly, C. Design of CompositeDrug Molecules: Mutual Effects on Binding to DNA of an Intercalator, Amsacrine, and a Minor Groove Binder, Netropsin. *Anti-Cancer Drug Des.* **1995**, *10*, 131–154.

(26) Bailly, C.; Denny, W. A.; Mellor, L. E.; Wakelin, L. P. G.; Waring, M. J. Sequence Specificity of the Binding of 9-Aminoacridine and Amsacrine-4-carboxamide to DNA Studied by DNase I Footprinting. *Biochemistry* **1992**, *31*, 3514–3524.

(27) Mrani, D.; Gosselin, G.; Auclair, C.; Balzarini, J.; De Clercq, E.; Paoletti, C.; Imbach, J. L. Synthesis, DNA Binding and Biological Activity of Oxazolopyridocarbazole–Netropsin Hybrid Molecules. *Eur. J. Med. Chem.* **1991**, *26*, 481–488.

(28) Herzyk, P.; Neidle, S.; Goodfellow, J. M. Conformation and Dynamics of Drug-DNA Intercalation. *J. Biomol. Struct. Dyn.* **1992**, *10*, 97–139.

(29) See, for example: Neidle, S.; Abraham, Z. Structural and Sequence-Dependent Aspects of Drug Intercalation into Nucleic Acids. *CRC Crit. Rev. Biochem.* **1984**, *17*, 73–121.

(30) (a) Wakelin, L. P. G.; Chetcuti, P.; Denny, W. A. Kinetic and Equilibrium Binding Studies of Amsacrine-4-carboxamides: a Class of Asymmetrical DNA-Intercalating Agents which Bind by Threading through the DNA Helix. *J. Med. Chem.* **1990**, *33*, 2039–2044. (b) Baguley, B. C. DNA Intercalating Anti-Tumour Agents. *Anti-Cancer Drug Des.* **1991**, *6*, 1–36.

(31) Matsumura, K. The Synthesis of Certain Acridine Compounds. *J. Am. Chem. Soc.* **1929**, *51*, 816–820.

(32) Jones, G. B.; Davey, C. L.; Jenkins, T. C.; Kamal, A.; Kneale, G. G.; Neidle, S.; Webster, G. D.; Thurston, D. E. The Non-Covalent Interaction of Pyrrolo[2,1-*c*][1,4]benzodiazepine-5,11-diones with DNA. *Anti-Cancer Drug Des.* **1990**, *5*, 249–264.

(33) (a) Manzini, G.; Barcellona, M. L.; Avitabile, M.; Quadrifoglio, F. Interaction of Diamidino-2-phenylindole (DAPI) with Natural and Synthetic Nucleic Acids. *Nucleic Acids Res.* **1983**, *11*, 8861–8876. (b) Marky, L. A.; Kupke, D. W. Probing the Hydration of the Minor Groove of A·T Synthetic DNA Polymers by Volume and Heat Changes. *Biochemistry* **1989**, *28*, 9982–9988.

(34) (a) Neidle, S.; Agbandje, M.; Jenkins, T. C.; McConnaughie, A. W. Structure and Conformational Features of 9-(4-Diethylaminophenyl)acridine. *Acta Crystallogr.* **1990**, *B46*, 860–862. (b) Walton, A. R.; Jenkins, T. C.; Neidle, S. Studies on 1,3-Diaryltriazene Analogues of Berenil: Molecules with Potential G·C Base-Pair Selectivity. *Acta Crystallogr.* **1991**, *B47*, 771–775.

(35) Lane, A. N.; Jenkins, T. C.; Brown, D. J. S.; Brown, T. NMR Determination of the Solution Conformation and Dynamics of the A·G Mismatch in the d(CGCAAATTGGCG)$_2$ Dodecamer. *Biochem. J.* **1991**, *279*, 269–281.

JM940689G